



# Investigation on potential and limitations of ERA5 Reanalysis downscaled on Italy by a convection-permitting model

Marianna Adinolfi<sup>1</sup> · Mario Raffa<sup>1</sup> · Alfredo Reder<sup>1</sup> · Paola Mercogliano<sup>1</sup>

Received: 15 November 2022 / Accepted: 18 April 2023 / Published online: 6 May 2023  
© The Author(s) 2023

## Abstract

This study presents a comprehensive assessment of a dynamical downscaling of ERA5 Reanalysis recently performed over Italy through the COSMO-CLM model at a convection-permitting scale ( $0.02^\circ$ ) over the period 1989–2020. Results are analysed against several independent observational datasets and reanalysis products. The capability of the downscaling to realistically represent the climatology for 2 m temperature and precipitation is analysed over the whole peninsula and subdomains. Hourly precipitation patterns, orography effects, and urban climate dynamics are also investigated, highlighting the weaknesses and strengths of the convection-permitting model. In particular, gains in performances are achieved in mountainous areas where the climate characteristics are correctly represented, as are the hourly precipitation characteristics. Losses in performances occur in coastal and flat areas of the Italian peninsula, where the convection-permitting model performance does not seem to be satisfactory, as opposed to complex orographic areas. The adopted urban parameterisation is demonstrated to simulate heat detection for two Italian cities: Rome and Milan. Finally, a subset of extreme climate indicators is evaluated, finding: (i) a region-dependent response, (ii) a notable performance of the convection-permitting model over mountainous areas and (iii) discrepancies in the South, Central and Insular subdomains. Climate indicators detect extreme events at a detailed scale, becoming an important tool for turning climate data into information.

**Keywords** Regional climate models · ERA5 reanalysis · Kilometer-scale resolution · Model evaluation · Urban parameterisation · Climate indicators

## 1 Introduction

In recent years, Italy, like other countries in the Mediterranean area, has been observing an increase in extreme weather events (i.e., heavy rainfall and increase in temperature), causing huge impacts (i.e., floods, droughts, heat waves) with consequences to assets and people (Amponsah et al. 2018; Gaume et al. 2009; Llasat et al. 2010; 2013). These occurrences are specifically related to peculiar characteristics of the region, such as demographic vulnerability (i.e., high-density population), orographic features, and the complex terrain close to the coast (Miglietta and Davolio 2022). Moreover, their occurrence in multiple climatic impact-drivers perspectives is expected to increase (with high confidence) since global warming is expected to

increase faster over this area than the global mean temperature change (IPCC 2021). Therefore, there is an increasing need for more reliable and detailed climate information on the Italian peninsula to improve the assessment of climate hazards and risk management.

Convection-permitting regional climate models (CP-RCMs) are increasingly considered a relevant step forward in studies for understanding past climate and climate change at local scales and extreme weather events that most impact society (Kendon et al. 2021), holding promising potentials (Prein et al. 2013). CP-RCMs have indeed highlighted added-value concerning the representation of precipitation, whether it concerns their spatial or temporal characteristics, particularly on the sub-daily time scale, especially in summer (Keller et al. 2016; Lind et al. 2016; Fowler et al. 2021). Several authors (Adinolfi et al. 2021; Ban et al. 2021; Berthou et al. 2020; Reder et al. 2020) demonstrated these improvements in complex orographic contexts, such as the Alpine area, also in the frame of different European projects and initiative as the European

✉ Marianna Adinolfi  
marianna.adinolfi@cmcc.it

<sup>1</sup> Fondazione Centro Euro-Mediterraneo Sui Cambiamenti Climatici, 81100 Caserta, Italy

Climate Prediction system-Horizon 2020 project (<https://www.eucp-project.eu/>) and the CORDEX Flagship Pilot Studies (Coppola et al. 2020) on Convective phenomena at high resolution over Europe and the Mediterranean (CORDEX FPS-CONV). The performances of CP-RCMs with “event-based” approaches for short-term statistics were tested in other studies (Coppola et al. 2020; Raffa et al. 2021b). Coppola et al. (2020) focused on three case studies indicating that large-scale driven events are captured in climate-mode even if the inter-model spread increases. Moreover, they argued the relevance of an ensemble-based approach to investigating high-impact convective processes. Raffa et al. (2021b) provided a reliable event-based analysis over two summer precipitation events in August 2007 and 2010 based on a direct downscaling of ERA5 (one-way nesting) at km-scale and a two-step nested one. The one-way nesting recognised the timing and intensity of the rainfall events. At the same time, the two-step nested one completely fails in their detection, possibly due to the influence of the lateral boundary condition by a freely evolving (i.e., not nudged) intermediate simulation allowing internal variability to develop.

Due to the previous promising outcomes of CP-RCMs, Raffa et al. (2021a) have released VHR-REA\_IT, a gridded hourly dataset over Italy for recent climate (January 1989 – December 2020) integrated into the CMCC Data Delivery System (DDS-<http://dds.cmcc.it> accessed on 4 August 2021). The VHR-REA\_IT dataset derives from the homonymous hindcast simulation that is the dynamical downscaling of ERA5 Reanalysis (Hersbach et al. 2020) at a convection-permitting scale ( $0.02^\circ$ , i.e.,  $\approx 2.2$  km). The dynamical downscaling has been performed with the COSMO-CLM (Consortium for Small-Scale Modeling in Climate Mode) Regional Climate Model (Rockel et al. 2008), switching on a specific module (i.e., TERRA-URB, Wouters et al. 2016) for modelling urban areas. VHR-REA\_IT exploits the added value of CP-RCMs for short-duration precipitation extremes, avoiding error-prone deep convection parameterisation schemes, which are sometimes responsible for misinterpreting precipitation patterns and trends (Kendon et al. 2021). It also brings with it the advantages of using urban parameterisation. This latter acts in synergy with the enhanced horizontal resolution, allowing for a better description of land-use dynamics related to the presence of cities (Gutowski et al. 2020), as well as increasing the relevance of activating specific urban canopy parameterisations (Wouters et al. 2016). Preliminary experiments (Garbero et al. 2021) have demonstrated the capability of the COSMO-CLM with TERRA-URB to reasonably detect the Urban Heat Island (UHI) effect and improve air temperature forecasts in different urban areas with specific morphological characteristics. Such capability provides relevant perspectives for enhancing urban climate modelling activities.

This paper presents an in-depth evaluation of the VHR-REA\_IT, highlighting the weaknesses and strengths of this dynamical downscaling of ERA5 at the convection-permitting scale. Furthermore, it aims to explore the capability of the hindcast simulation to represent the climatology of average and extreme patterns of temperature and precipitation in a manner consistent with different independent observation datasets. The overall goal of the paper is to highlight some steps forward in comparison with state-of-the-art:

- (i) providing climate information with increased space ( $\approx 2.2$  km) and time (1 h) resolutions;
- (ii) exploiting the potential of convection-permitting models and urban parameterisation to represent the past and current climate synergically;
- (iii) characterising on a detailed scale extreme events having the potential for significant negative impacts on lives, infrastructure or the environment (Fowler and Ali 2022)

Specific analyses focus on the hourly precipitation features, orography effects, and urban dynamics. Moreover, extreme events are investigated considering a subset of indices for precipitation and temperature of the World Meteorological Organization (WMO) Expert Team on Climate Change Detection and Indices (ETCCDI).

The paper is organized as follows. First, Sect. 2 introduces the regional climate model with initial and boundary conditions, VHR-REA\_IT setup details, the observations and reanalysis products assumed as reference for evaluation, and the evaluation method considered for analysing extremes. Section 3 presents and discusses the evaluation results for temperature and precipitation, as regard mean characteristics (i.e., spatial patterns, orography effects) and extremes, giving evidence of specific peculiarities in urban dynamics and hourly precipitation patterns. Section 4 draws conclusions.

## 2 Model, data and methods

### 2.1 Regional Climate Model COSMO-CLM and set-up

VHR-REA\_IT has been performed by dynamically downscaling ERA5 Reanalysis at  $0.02^\circ$  ( $\approx 2.2$  km) with the regional climate model COSMO-CLM (Rockel et al. 2008). It is a non-hydrostatic and limited-area model designed for dynamically downscaling simulations at different horizontal resolutions varying from the meso- $\beta$  (horizontal scales in-between 20–200 km) to the meso- $\gamma$  (horizontal scales in-between 2–20 km). It exploits finite difference methods to solve fully compressible governing equations of

fluid dynamics on a structured grid using finite difference methods.

Horizontal advection is calculated using a fifth-order upwind scheme, and vertical advection is computed with an implicit Crank–Nicholson scheme (Förstner and Doms 2004). Time integration is performed with a split-explicit third-order Runge–Kutta discretisation (Baldauf et al. 2011). Cloud microphysics is represented with a single-moment scheme (Doms and Baldauf 2011) using five hydrometeors (cloud water, rain, ice crystals, snow, and graupel). The radiation scheme is based on a  $\delta$  two-stream approach described by Ritter and Geleyn (Ritter and Geleyn 1992).

Turbulent fluxes within the planetary boundary layer are parameterised with a 1.5-order turbulent kinetic energy (TKE)-based scheme (Mellor and Yamada, 1982; Raschendorfer 2001). The standard parameterisation of convection used in the model is based on the Tiedtke scheme (Tiedtke 1989), a mass-flux closure approach used to parameterise modifications to the vertical structure of the atmosphere due to deep, midlevel and shallow convection. In convection-permitting mode, the deep convection is explicitly resolved; therefore, only the shallow convection part of the scheme is active.

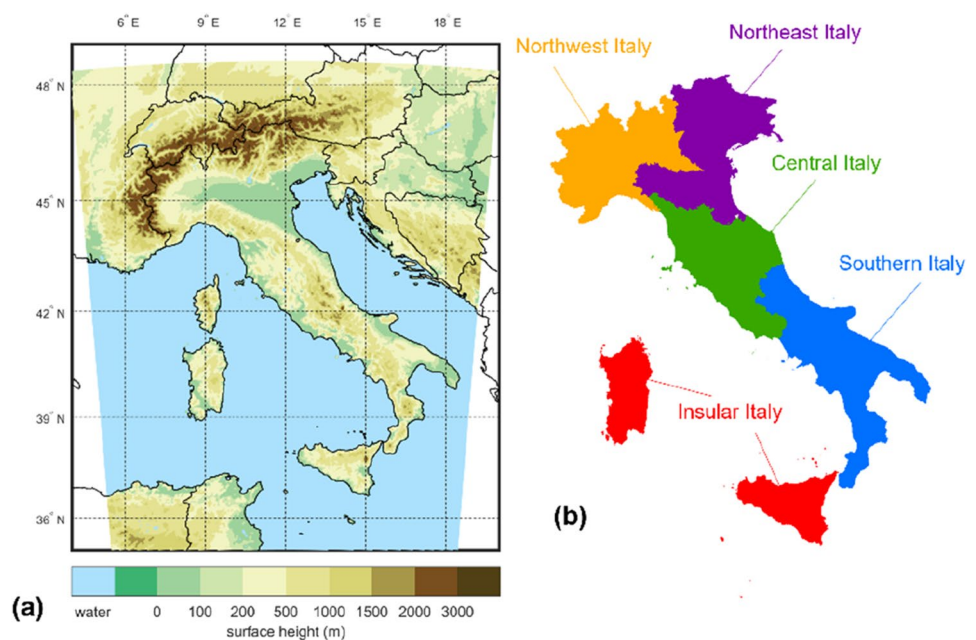
The representation of soil moisture is performed using a 7-layer soil model (TERRA\_ML) with a formulation for water runoff dependent on orography (Schrodin and Heise 2001). COSMO-CLM also allows turning on an intrinsic representation of urban physics by employing TERRA-URB parameterisation (Wouters et al. 2016) with a bulk scheme to discern each grid cell between urban canopy and natural land cover and computes adjusted soil and water fluxes considering the urban environment features.

The VHR-REA\_IT dynamical downscaling relies on the COSMO-DE model configuration developed by the Deutscher Wetterdienst for numerical weather prediction application. Such a configuration has been modified adequately in Raffa et al. (2021a) to account for the urban effects, switching on the TERRA-URB parameterisation, and to solve convection explicitly as in the frame of the CORDEX FPS-CONV initiative.

The simulation was performed on the supercomputer cluster GALILEO available at the Consorzio Interuniversitario del Nord-Est per il Calcolo Automatico (CINECA) using the version COSMO-CLM 5.00\_clm9 associated with the interpolator version int2lm\_2.00\_clm4. It has been initialised and driven by the ERA5 reanalysis (Hersbach et al. 2020) of the European Centre for Medium-Range Weather Forecast (ECMWF) using a direct downscaling strategy as described in Raffa et al. 2021b. ERA5 currently represents the most plausible climate descriptor suitable for several applications, such as monitoring climate change, research, education, policy-making, and business. It has a global coverage with a spatial resolution of  $0.28^\circ$  ( $\approx 31$  km) and provides outputs at an hourly scale from 1950 to the present. Recently, several dynamical downscaling experiments (Reder et al. 2022; Wang et al. 2021; Pilguy et al. 2022) relied on initial and boundary conditions from ERA5, being assumed as the reference reanalysis for the experiment design of the dynamical downscaling of the Coupled Model Intercomparison Project Phase 6 (CMIP6) global models generation over the EURO-CORDEX domain.

The computational domain (Lon =  $5^\circ\text{W}$ – $20^\circ\text{E}$ ; Lat =  $36^\circ\text{N}$ – $48^\circ\text{N}$ ; see Fig. 1a) consists of  $585 \times 730$  grid points, 50 vertical levels and 7 soil levels. The analysis domain is

**Fig. 1** **a** Surface height (m a.s.l.) of the computational domain; **b** area considered for validation defined according to the first level of Nomenclature of Territorial Units for Statistics (NUTS 1) for Italy



obtained by discarding the relaxation zone from the computational domain (25 points for each border). The covered period is 1989–2020, assuming the year 1988 as spin-up. Its time step for integration based on a third-order Runge-Kutta scheme is 20 s.

The external datasets adopted in VHR-REA\_IT are GLC2000 (Bartholomé and Belward 2005) for land use, GLOBE for surface elevation, and FAO Digital Soil Map of the World for soil types. Moreover, additional external datasets are the impervious surface area obtained from the European Environment Agency (Maucha et al. 2010) and the anthropogenic heat flux for the year 2006 derived by Flanner (2009), as TERRA-URB is activated.

## 2.2 Observations and reanalysis products

As the resolution of climate models increases, the evaluation of CP-RCM simulations becomes challenging due to the lack of high-quality and high-resolution observational gridded datasets (Piazza et al. 2019). Moreover, despite being all based on meteorological stations, a large discrepancy between the different observed gridded datasets has been highlighted (Zittis et al. 2017). This is especially true in areas with low population density (i.e., islands) and mountainous regions where weather stations are sparsely distributed and precipitation undercatches snowfall in winter.

In the previous study (Raffa et al. 2021a), the VHR-REA\_IT dataset was validated against the observational dataset E-OBS (Cornes et al. 2018). The main findings of this evaluation are also reported in the following figures and discussion of the results in order to depict a comprehensive evaluation of the hindcast simulation. In this work, VHR-REA\_IT has been evaluated against different independent observational datasets available for Italy. Specifically:

- E-OBS (Cornes et al. 2018; Haylock et al. 2008): represents a daily gridded European land-only observational dataset at a horizontal resolution of  $0.1^\circ$  ( $\sim 11$  km) relying on the “blended” time series from the station network of the European Climate Assessment & Dataset (ECA&D) project. It contains data for precipitation amount, mean/maximum/minimum temperature, relative humidity, sea level pressure, and surface shortwave downwelling radiation. Its latest version (version 25.0e), delivered by Copernicus Climate Data Store, covers the period 1950–2021.
- SCIA-ISPRA (Desiato et al. 2011): is a daily gridded dataset of the Italian Environmental Protection Agency (ISPRA), available at a horizontal resolution of approximately 5 km for maximum and minimum temperatures and 10 km for rainfall. This dataset is derived by interpolating data from local weather stations (LWS). It

covers the twentieth century to the present day, with varying reliability due to the number of interpolated values available each year.

- GRIPHO (Fantini 2019): is an hourly gridded dataset for precipitation, available at a horizontal resolution of around 10 km. This dataset is based on rain gauge measurements for 2001–2016 and is open to CORDEX FPS-CONV members through a UNESCO ICTP personal communication.

In addition, in order to overcome the discrepancies among different observational gridded datasets, VHR-REA\_IT is also compared with reanalysis products as ERA5 (the driven reanalysis of VHR-REA\_IT as detailed in §2.1) and UERRA. Specifically:

- ERA5 (Hersbach et al. 2020): is the fifth-generation ECMWF reanalysis representing the most plausible description of the current climate nowadays. It has global coverage with a spatial resolution of  $0.25^\circ$  ( $\approx 31$  km) and provides hourly outputs from 1950 to the present (with a latency of 5 days). Such features make ERA5 suitable for a wide range of applications, such as monitoring climate change, research, education, policy-making and business in sectors such as renewable energy and agriculture (Buontempo et al., 2020). It forms the basis for monthly C3S climate bulletins. It is used in the World Meteorological Organization’s annual assessment of the State of the Climate presented at the Conference of the Parties of the United Nations Framework Convention on Climate Change (UNFCCC). ERA5 data are available as hourly and monthly products on pressure levels (upper air fields), model and single levels (atmospheric, ocean-wave and land surface quantities).
- UERRA (MESCAN-SURFEX option-Gustafsson et al. 2001; Ridal et al. 2017; Bazile et al. 2017): is a reanalysis at  $\sim 5.5$  km, providing estimations of the climate in Europe for the period 1961–2019, obtained by combining the UERRA-HARMONIE and the MESCAN-SURFEX systems. UERRA-HARMONIE is a regional reanalysis ( $\sim 11$  km) over Europe based on a 3-dimensional variational data assimilation system. In addition to observations in the model domain, it assimilates along the lateral borders data from ERA40 (until the end of 1978) and ERA-Interim (from 1979). MESCAN-SURFEX is a complementary surface analysis system forced by the UERRA-HARMONIE reanalysis. Using the Optimal Interpolation method, it provides daily accumulated precipitation and six-hourly air temperature and relative humidity at two meters above the model topography.



## 2.3 Methods for the evaluation

This study investigates the performances of VHR-REA\_IT for temperature and total precipitation. To this aim, independent observational datasets such as SCIA-ISPRA, E-OBS and GRIPHO (see §2.2) have been assumed as references. SCIA-ISPRA and E-OBS are used as a baseline for temperature and precipitation on the daily scale across the period 1989–2020. For SCIA-ISPRA, the daily mean temperature is the average value between daily minima and maxima values (Allen et al. 1998). The daily mean temperature thus obtained for SCIA-ISPRA only provides a rough estimate, as the variable of daily average temperature is used directly for other datasets. GRIPHO is adopted to evaluate precipitation at the hourly scale for the entire available period (2001–2016).

For both variables, the evaluation is first conducted by comparing observations and simulation in terms of spatial distributions through maps; the qualitative comparison is then turned into quantitative information using specific metrics (i.e., bias and variability) computed at annual and seasonal scales to corroborate the analyses. Moreover, a comparison with reanalysis products such as ERA5 (the driven reanalysis of VHR-REA\_IT) and UERRA (see §2.2) have been performed thorough maps and metrics able to assess the added value. In particular, the DAV metric (Soares and Cardoso 2018) provides an objective and normalized measure of the added value in terms of potential gain in the performance of climate models due to the usage of a higher resolution, comparing higher- and coarser-resolution simulation probability density function (PDFs) to the observational PDF (Cardoso and Soares 2022; Careto et al. 2022; Tölle and Churiulin 2021). DAV accounts for the difference in skill scores between high resolution (*hr*) and low resolution (*lr*), assuming the observations (*obs*) as reference: (1) where  $S_{hr}$  and  $S_{lr}$  are the Perkins skill scores for high and low

resolution respectively;  $n$  is the number of bins considered to obtain the PDF;  $Z_{hr}$ ,  $Z_{lr}$  and  $Z_{obs}$  are the frequencies of values in each bin for high resolution, low resolution, and observations respectively. Specifically, the Perkins skill score is a quantitative measure of how well each simulation resembles the observed probability density functions by measuring the common area between two probability density functions (Perkins et al. 2007). In general,  $DAV = 0$  indicates that no gain is found;  $DAV < 0$  points out a loss associated with using a higher resolution relative to the lower resolution;  $DAV > 0$  expresses the beneficial impact of increasing the grid spacing.

In a second step, more detailed information is provided, assuming the Nomenclature of Territorial Units for Statistics (NUTS1) classification 2021 (Fig. 1b) as the spatial reference. NUTS1 for Italy splits the peninsula into five sub-areas (i.e., Northwest Italy, Northeast Italy, Central Italy, South Italy, and Insular Italy). For each sub-area, the evolution of the annual bias, the orography role, and the assessment of extremes through climate indicators are investigated. To address the orography role, the 30-year mean temperature and precipitation values are first grouped into 300-metre orographic bands and then averaged. Such an operation has been performed for observations and simulation independently. The evaluation of extremes relies on climate indicators for temperature and precipitation (see Table 1), selected among those provided by the experts of the CCI/CLIVAR/JCOMM Team on Climate Change Detection and Indices (ETCCDI; Karl et al. 1999). These indicators generally turn climate data into information highlighting various characteristics of extremes, including frequency, amplitude, and persistence. In this work, some indicators are used following the precise definition provided by ETCCDI, although others are slightly modified from the originals. Operatively, some frequency indicators (i.e., FD, SU, TR, R20mm, CWD and CDD) are calculated yearly and then averaged over 30-year;

**Table 1** List of indicators chosen for temperature and precipitation

Description of climate indicators for temperature	Label	Units
90th percentile of daily maximum temperature	TX90th	°C
10th percentile of daily minimum temperature	TN10th	°C
Annual count of days when the daily minimum temperature is below 0 °C	FD	day/y
Annual count of days when the daily maximum temperature is above 25 °C	SU	day/y
Annual count of days when the daily minimum temperature is above 20 °C	TR	day/y
Description of climate indicators for precipitation	Label	Units
Maximum of daily precipitation	RX1d	mm/d
99th percentile of daily precipitation considering only the wet days with daily precipitation greater than 1 mm	R99th	mm/d
Number of days with precipitation greater or equal to 20 mm	R20mm	day/y
Maximum number of consecutive wet days with daily precipitation greater than 1 mm	CWD	day/y
Maximum number of consecutive dry days with daily precipitation lower than 1 mm	CDD	day/y

others, such as the percentiles and the absolute indicators (i.e. TX90th, TN10th, RX1d and R99th), are instead calculated considering the entire distribution of values for the 30-year.

Once calculated, each indicator is spatially aggregated at the NUTS1 level (see Fig. 1b), deriving spatial mean and spread between the 5th and 95th percentile of the spatial distribution. The outcomes are displayed using a “radar chart” representation.

Then, further separate analyses are performed for temperature and precipitation, focusing on the summer season (JJA). Maps of minimum temperature, normalised using the Min-Max procedure (Patro and Sahu 2015), are proposed for the two biggest Italian cities (i.e., Milan and Rome) to preliminarily appreciate the model’s ability to capture the UHI phenomena. In this application, measurements from LWS (on which SCIA-ISPRA relies) are processed with the Ordinary Kriging technique (Wackernagel 1995) and assumed as the baseline. On the other hand, for precipitation, hourly maps of intensity, frequency, and heavy precipitation are presented to verify the potential benefits of the CP-RCM. Specifically, intensity and frequency are assessed on wet hours (an hour with precipitation  $\geq 0.1$  mm/h). In contrast, heavy hourly precipitation is investigated through the amount of hourly precipitation above the 99.9th percentile computed from all data (wet and dry events), according to Schär et al. (2016). The amount of hourly precipitation is also investigated using whiskers and box plot representations to look for differences in the statistical distributions synthetically: the halfway mark indicates the median, and the bottom and top edges of the box indicate the 25th and 75th percentiles, respectively. Moreover, diurnal cycles averaged over NUTS1 are assessed during summer for wet-hour frequency and intensity.

### 3 Results and discussion

#### 3.1 Assessments of temperature and related extremes

##### 3.1.1 General temperature features

Figure 2 displays the spatial distribution of daily mean temperature over 1989–2020 from SCIA-ISPRA (Fig. 2a), E-OBS (Fig. 2b), UERRA (Fig. 2c), ERA5 (Fig. 2d) and VHR-REA\_IT (Fig. 2e), on their native grids. Data from UERRA refer to 1989–2019.

It figures out a general good ability of the climate simulation in reproducing observational spatial patterns. In particular, the simulated 2m temperature agrees with observations (both SCIA-ISPRA and E-OBS) over the Alps and Apennine chains and the mountainous areas in southern Italy (

as Basilicata, Calabria, and the Etna volcano). On the other hand, the simulation slightly overestimates temperature over flat terrains such as the Po valley, northwestern Italy (as South Piemonte), and coastal areas, especially if compared with E-OBS. Several studies found a temperature overestimation in the Po valley due to a typical atmospheric dynamic acknowledged as surface-based temperature inversions (Cacciamani et al. 1995; Bucchignani et al. 2016) not reproduced by most climate models.

Yearly statistics (i.e. mean values and standard deviations) shown in Figure 2 and reported in Table 2, confirm the good agreement between observations and VHR-REA\_IT. Specifically, the yearly mean value for observations is 13.2 °C for SCIA-ISPRA and 13.1 °C for E-OBS, with a spatial variability of  $\pm 3.8$  °C for both observational datasets. In comparison, it is 13.7 °C for VHR-REA\_IT with a spatial variability of  $\pm 4.2$  °C. UERRA and ERA5 show a yearly mean value of 12.5 °C and 12.9 °C, respectively, with a spatial variability of  $\pm 3.7$  °C and  $\pm 3.9$  °C, respectively. By looking at seasonal values (see Table 2), VHR-REA\_IT against SCIA-ISPRA returns a cold bias (−1.2 °C) during winter and a warm tendency (+1.8 °C) during summer. In contrast, the biases are attenuated during the transition seasons (i.e., autumn and spring, with values = +0.1 °C and +0.5 °C, respectively). Such a tendency also emerged in the seasonal comparisons against E-OBS (also reported in Raffa et al. 2021a), highlighting cold winter bias and warm summer bias. Similar tendencies occur in the comparison of VHR-REA\_IT against UERRA and ERA5. The overestimation of VHR-REA\_IT in summer temperature may be related to the soil moisture-precipitation feedback modification (Pielke 2001; Koster et al. 2004) acting when an explicit treatment of deep-convection processes is turned on (Hohenegger et al. 2009; Taylor et al. 2013). Indeed, a different soil moisture-precipitation feedback influences the heat flux partitioning, affecting summer temperature. Such behaviour seems to be revealed by several CP-RCMs, as highlighted in Sangelantoni et al. (2023).

Moreover, the spatial patterns in Figure 2 show that UERRA reanalysis slightly underestimates 2m temperature over the whole domain if compared with SCIA-ISPRA observations fitting in a good way E-OBS, whereas ERA5 patterns are in better agreement with SCIA-ISPRA than E-OBS, especially over flat terrain. Such qualitative analyses about the reanalysis products performance are also confirmed by the DAV metric reported in Table 3, where SCIA-ISPRA is used as the reference. Generally, DAV assessed over Italy indicates an added value in VHR-REA\_IT of 14% if compared with UERRA reanalysis and a slight loss of −4% if compared with ERA5. The DAV over NUTS1 indicates that an added value in VHR-REA\_IT is found considering both UERRA and ERA5 over Insular, Central and Southern areas. In contrast, slight losses are quantified over Northern

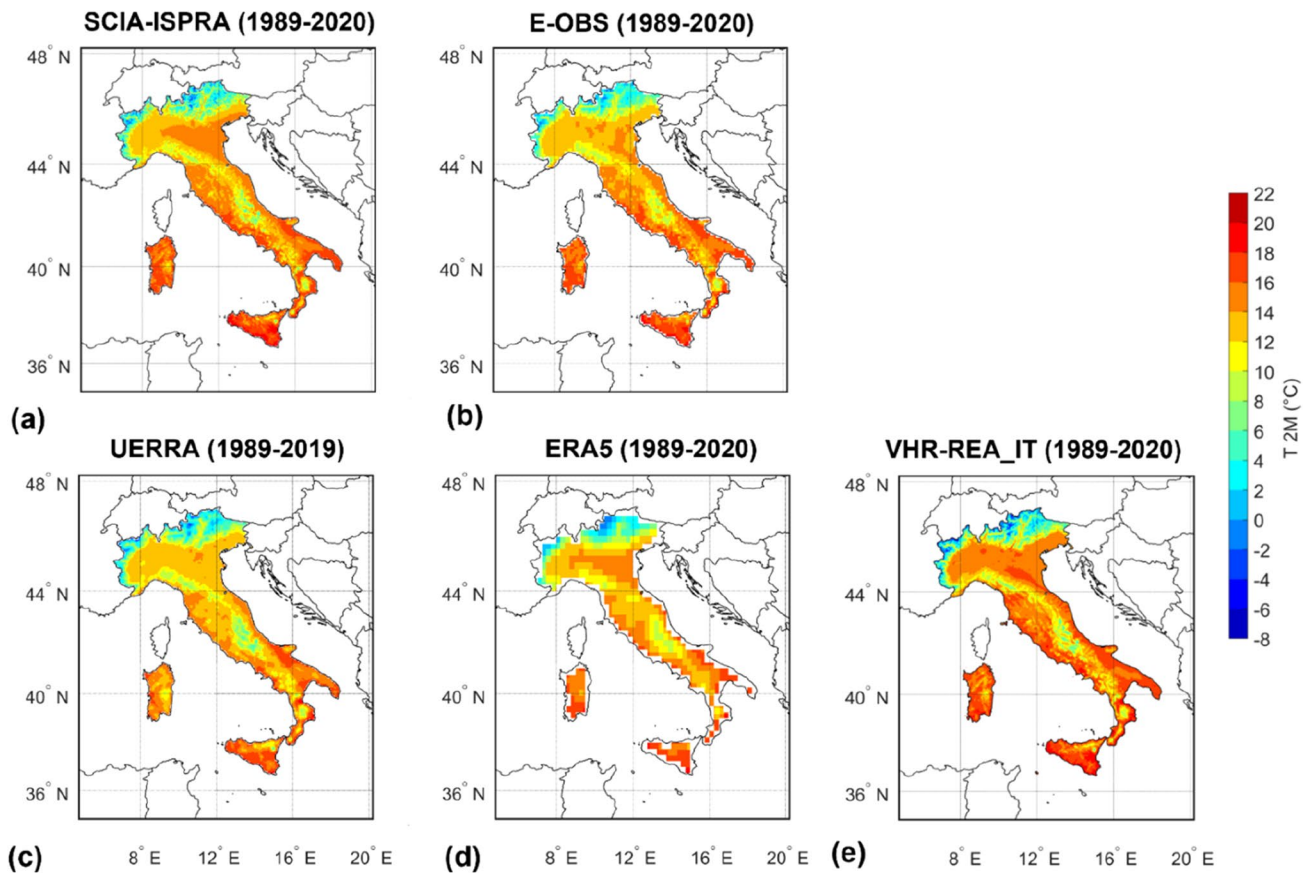


**Fig. 2** Spatial distribution of daily mean temperature from SCIA-ISPRA (a), E-OBS (b), UERRA (c), ERA5 (d) and VHR-REA\_IT (e) over 1989–2020 (except for UERRA covering the period 1989–2019)

**Table 2** Metrics (mean value and standard deviation) over the whole domain from SCIA-ISPRA, E-OBS, UERRA, ERA5 and VHR-REA\_IT related to the 2 m temperature spatial distribution for the period 1989–2020

	SCIA-ISPRA	E-OBS	UERRA	ERA5	VHR-REA_IT
YEARLY (°C)	13.2 (± 3.8)	13.1 (± 3.8)	12.5 (± 3.7)	12.9 (± 3.9)	13.7 (± 4.2)
SON (°C)	14.3 (± 2.1)	13.9 (± 4.1)	13.1 (± 3.9)	13.8 (± 4.1)	14.4 (± 4.4)
DJF (°C)	5.8 (± 2.5)	5.3 (± 4.1)	4.5 (± 3.9)	4.8 (± 4.7)	4.6 (± 4.1)
MAM (°C)	11.8 (± 2.5)	11.7 (± 3.6)	11.2 (± 3.5)	11.6 (± 3.6)	12.3 (± 4.2)
JJA (°C)	21.5 (± 2.3)	21.4 (± 3.8)	21.1 (± 3.9)	21.5 (± 3.6)	23.3 (± 4.5)

Metrics are yearly and seasonally (*SON* September–October–November, *DJF* December–January–February, *MAM* March–April–May, *JJA* June–July–August) reported

areas, mainly due to temperature overestimation of VHR-REA\_IT in the Po Valley.

In addition, Figure 3 shows the yearly evolution of 2m temperature bias over NUTS1 subdomains. Such elaboration confirms a warm bias for each NUTS with values between 0.4 and 1.4 °C. The lower limit of this bias is in the North-west area. It is also interesting to note the evolution of the bias in the Insular area, where the trend over time is in line with the other regions from 2003 onwards. In contrast, the evolution appears to be inconsistent in previous years. It may be due to the low potential reliability of LWS observations

on which the SCIA-ISPRA grid relies. This point would need further investigation.

### 3.1.2 Orography effects

Figure 4 shows the altitudinal profiles of mean temperature obtained for each NUTS1 (Fig. 4a–e) using SCIA-ISPRA and VHR-REA\_IT on their native grids. Observations show an expected reduction in temperature with increasing altitude. The simulation reproduces such a reduction with slight differences for altitude values > 1500 m. The average lapse

**Table 3** DAV metric for 2 m temperature assessed over Italy (whole domain) and over NUTS1 from VHR-REA\_IT (as high resolution product), SCIA (as observation), UERRA and ERA5 (as low resolution product), respectively

NUTS1	DAV—UERRA (%)	DAV—RA5 (%)
Italy (whole domain)	14	−4
Northwest	−9	−16
Northeast	−7	−1
Central	21	7
South	14	22
Insular	51	29

rate in the case of observations is about  $-5.7\text{ }^{\circ}\text{C}/1000\text{m}$ , with the steepest value in Southern Italy ( $-6.0\text{ }^{\circ}\text{C}/1000\text{m}$ , see Fig. 4d) and the lowest one in Insular Italy ( $-5.1\text{ }^{\circ}\text{C}/1000\text{m}$ , see Fig. 4e). VHR-REA\_IT returns slightly steeper lapse rate values than the observations, with an average value of about

$-6.4\text{ }^{\circ}\text{C}/1000\text{m}$  becoming  $-6.7\text{ }^{\circ}\text{C}/1000\text{m}$  in the South (see Fig. 4d) and North-East (see Fig. 4b), and  $-6.0\text{ }^{\circ}\text{C}/1000\text{m}$  in Insular Italy (see Fig. 4e). This analysis has been performed by considering the distribution of altitudes related to each dataset. Such assumption makes the results at higher altitudes affected by a degree of uncertainty (in any case reduced) due to the limited number of grid points considered for SCIA-ISPRA. In any case, the lapse rates returned by the observations and VHR-REA\_IT aligns with the altitudinal thermal gradient theoretically calculated in the standard atmosphere and equal to  $-6.5\text{ }^{\circ}\text{C}/1000\text{m}$  (Cavcar 2000).

### 3.1.3 Mapping of urban heat during summer nights

The increase in built surfaces constitutes the main reason for the formation of urban heat, as urban canyons preclude the release of reflected radiation. The main contribution to the formation of urban heat is the missing night-cooling of horizontal surfaces, together with a cloudless sky and light

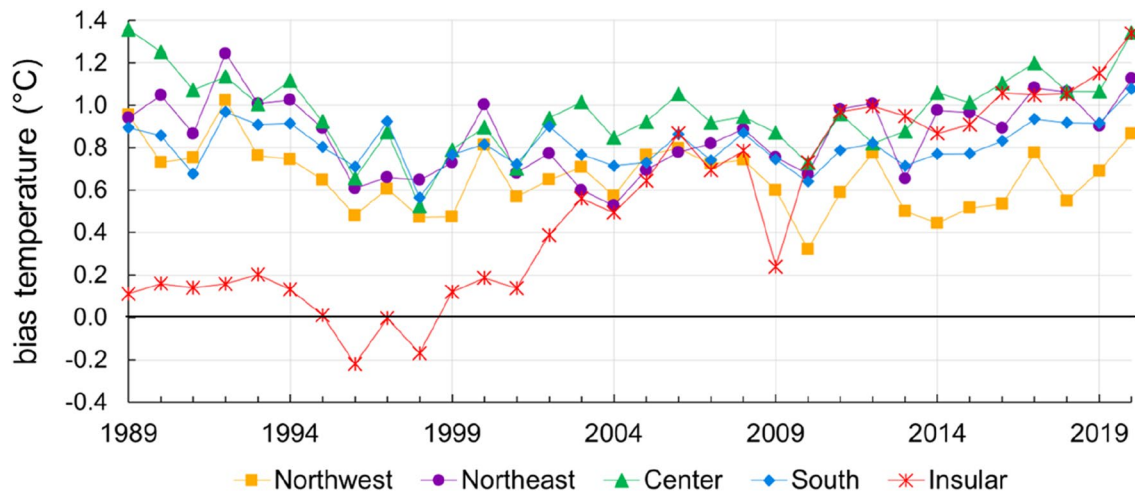


**Fig. 3** Evolution of the annual bias of VHR-REA\_IT against SCIA-ISPRA dataset of 2 m mean temperature over NUTS1

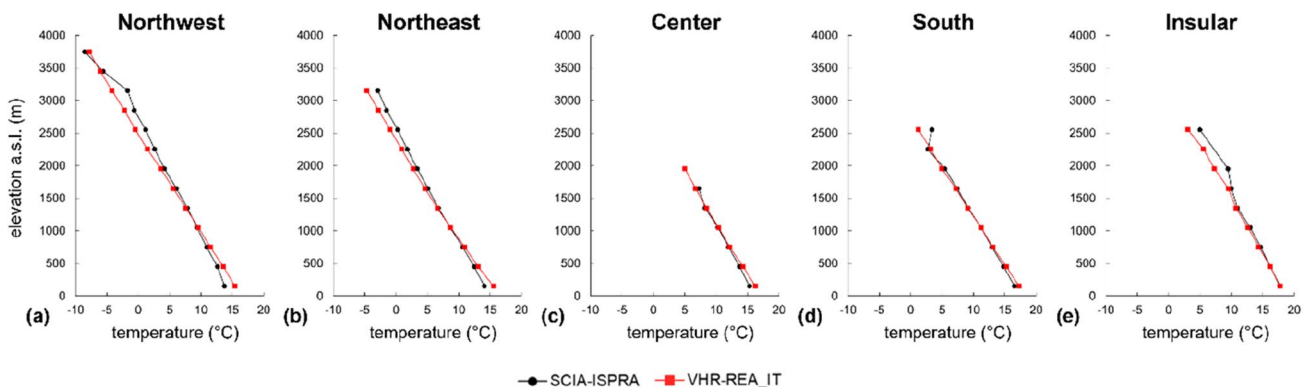


**Fig. 4** Altitudinal profiles of mean 2 m temperature obtained for each NUTS1 (subplots a-e) using SCIA-ISPRA (black line) and VHR-REA\_IT (red line)



winds (Oke et al. 2017). Of course, there is also a contribution from indoor heating, vehicle presence, and waste heat from air conditioning and refrigeration systems. The COSMO-CLM model can cope with this effect by modelling urban environments with the bulk parameterisation scheme (i.e., TERRA-URB), exploiting prescribed anthropogenic heat flux, impervious surface area, and other external urban canopy parameters (Garbero et al. 2021). In general, cities store a high amount of heat during the daylight hours warming the town elements (i.e., roads, walls and roofs) that release this trapped heat during the night hours, warming the air within the town. Therefore, the released heat is maximised during the summer night hours (Reder et al. 2018). So the analyses on the minimum temperatures are proposed in the following associated with tropical night occurrence.

Figure 5 shows the maps of minimum temperature, normalised using the Min-Max procedure, for the cities of Milan (Fig. 5a for observation SCIA\_ISPRA LWS, Fig. 5b for reanalysis product ERA5 and Fig. 5c for the simulation) and Rome (Fig. 5d for observations SCIA\_ISPRA LWS, Fig. 5e for reanalysis product ERA5, and Fig. 5f for the simulation) to track the urban heat during summer nights. The Min-Max procedure is a normalisation method by performing linear transformations of the original data (Kappal 2019). Specifically, the minimum value of data is transformed into 0 while the maximum to 1 so that other values gets transformed into a decimal between 0 and 1.

Observations capture the urban heat island effect, gradually disappearing as it moves away from the more urbanised

area. ERA5, also due to its coarse resolution, is not able to reproduce the urban heat island effect while the results of the dynamical downscaling consistently highlight the ability of urban parameterisation to represent urban dynamics and thermal peculiarities compared to observations. This result is particularly evident for Milan. Finally, it is interesting to note that the warm blob detected by VHR-REA\_IT (Fig. 5f) and identified with the triangular symbol, is due to the presence of a body of water (i.e. the Lake Bracciano) which reduces the diurnal air temperature variation (i.e., maximum and minimum temperature close to the mean value), returning higher minimum temperature than that of the areas surrounding the city.

### 3.1.4 Extreme temperature indicators

The last section for temperature evaluation focuses on analysing extreme temperature indicators introduced in §2 and listed in Table 1. Figure 6 shows the temperature-related ETCCDI climate indicators for 1989–2020 represented through the radar chart for each NUTS1. The plots provide mean (continuous line), 5th percentile (filled circle) and 95th percentile (filled square) values of indicators allowing the comparison between the VHR-REA\_IT and SCIA-ISPRA datasets. The values are also provided in Table 4 as mean value differences between VHR-REA\_IT and SCIA-ISPRA.

VHR-REA\_IT generally overestimates the 90th percentile of daily maximum temperature (TX90th, see Fig. 6a) against SCIA-ISPRA observations with almost uniform

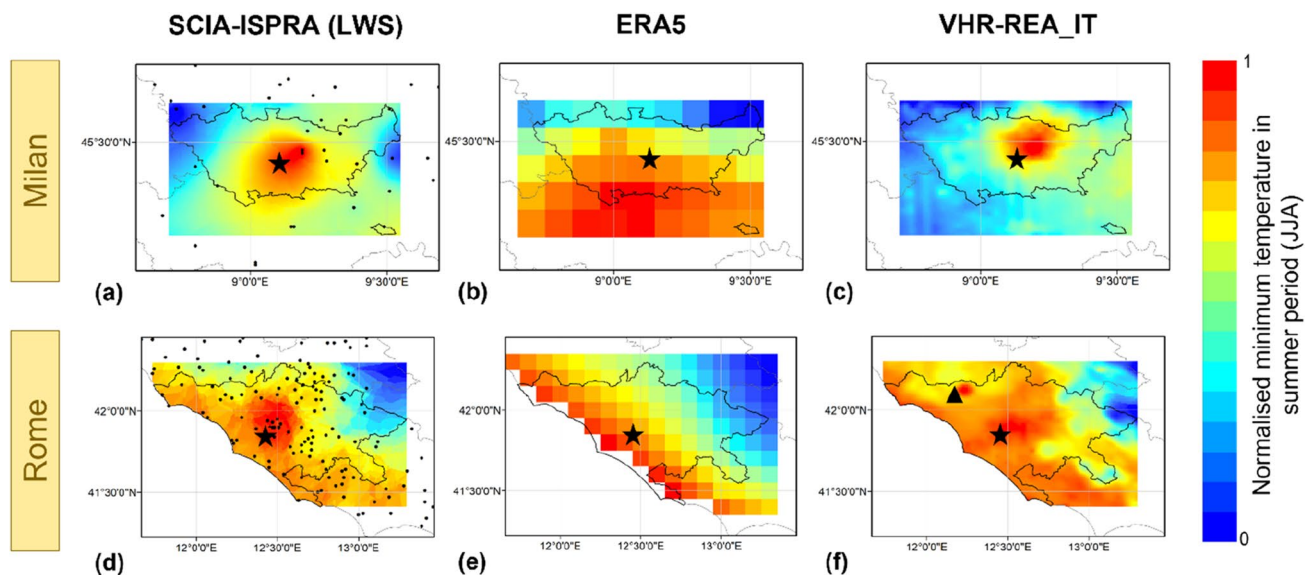


**Fig. 5** Spatial patterns of the minimum temperature during summer (representative of night-time conditions) over Milan urban context retrieved by SCIA-ISPRA local weather stations (a), ERA5 (b) and VHR-REA\_IT (c). Respectively subplots (d), (e) and (d) refers to Rome urban context. Minimum temperature in JJA have been normal-

ised respect to their relative maxima values. Local weather stations (LWS) are localized in subplots (a) and (d) and represented by filled black circles. Star symbol indicates the urban centre while the triangular symbol locates the Bracciano lake

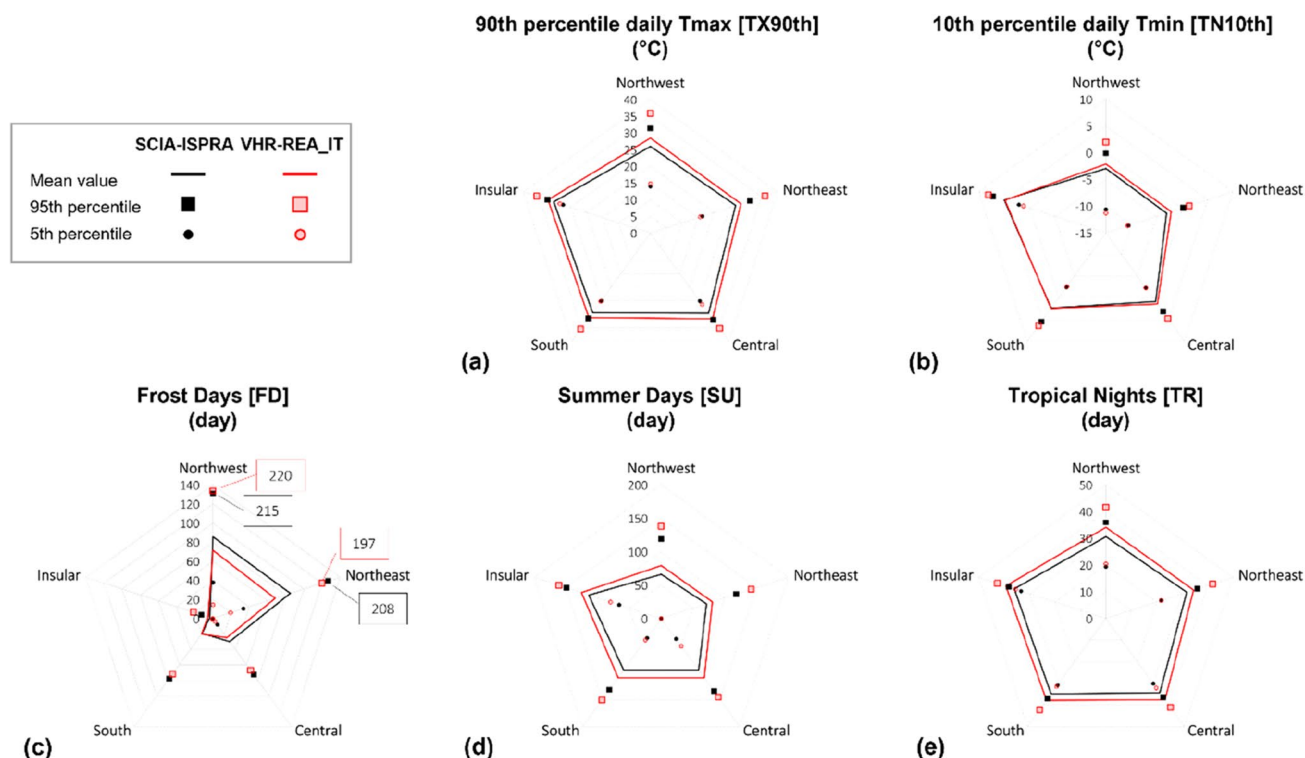


**Fig. 6** Radar chart for temperature-related ETCCDI climate indicators for 1989–2020 for each NUTS1. The plots provide mean (continuous line), 5th percentile (filled circle) and 95th percentile (filled square) values of indicators allowing the comparison between the

VHR-REA\_IT (red lines and fills) and SCIA-ISPRA (black lines and fills) datasets. The retrieved climate indicators are: 90th percentile daily Tmax—TX90th (a), 10th percentile daily Tmin—TN10th (b), frost days—FD (c), Summer days—SU (d) and tropical nights -TR (e)

values overall NUTS1. The same occurs for the 10th percentile of daily minimum temperature (TN10, see Fig. 6b), with nearly similar values over all NUTS1, except over the Insular area exploiting the highest TN10th. Concerning frost days (FD, see Fig. 6c), VHR-REA\_IT slightly underestimates this indicator against observations. This outcome is mainly due to the warm bias featuring VHR-REA\_IT. The distribution is non-uniform along NUTS1, with the lowest values yielded over the Insular and Southern areas where FD are rare. VHR-REA\_IT tends to overestimate the number of summer days (SU, see Fig. 6d) with almost uniform

values over all NUTS1, except for the Insular area returning the highest value among NUTS1. Finally, for the number of tropical nights (TR, see Fig. 6f), VHR-REA\_IT returns higher values than SCIA-ISPRA observations. Again, these values are almost uniform over all NUTS1.

To sum up, the indicators TX90th and TN10th are uniform and well reproduced by VHR-REA\_IT. The same is for summer days and tropical nights. A response dependent on the region, especially in topographically complex areas, is performed by frost days magnifying differences between Northern and Southern areas, resulting in a non-uniform radar plot.

**Table 4** VHR-REA\_IT minus SCIA-ISPRA mean values of the selected climate indicators for temperature over NUTS1

	Northwest	Northeast	Central	South	Insular
TX90th (°C)	2	1	2	2	2
TN10th (°C)	1	1	0	0	0
FD (%)	−17%	−20%	−17%	5%	67%
SU (%)	20%	13%	15%	16%	10%
TR (%)	43%	41%	33%	25%	16%

Values are reported as absolute bias (model-observation) for TX90th and TN10th and percentage bias (model-observation)/observation for FD, SU and TR

### 3.2 Assessment of precipitation and related extremes

#### 3.2.1 General precipitation features

Figure 7 shows the spatial distribution of daily mean precipitation from SCIA-ISPRA (Fig. 7a), E-OBS (Fig. 7b), GRIPHO (Fig. 7c), UERRA (Fig. 7d), ERA5 (Fig. 7e) and VHR-REA\_IT (Fig. 7f) on their native grids. Data from SCIA-ISPRA, ERA5, E-OBS and VHR-REA\_IT refer to 1989–2020, data from UERRA refer to 1989–2019, while

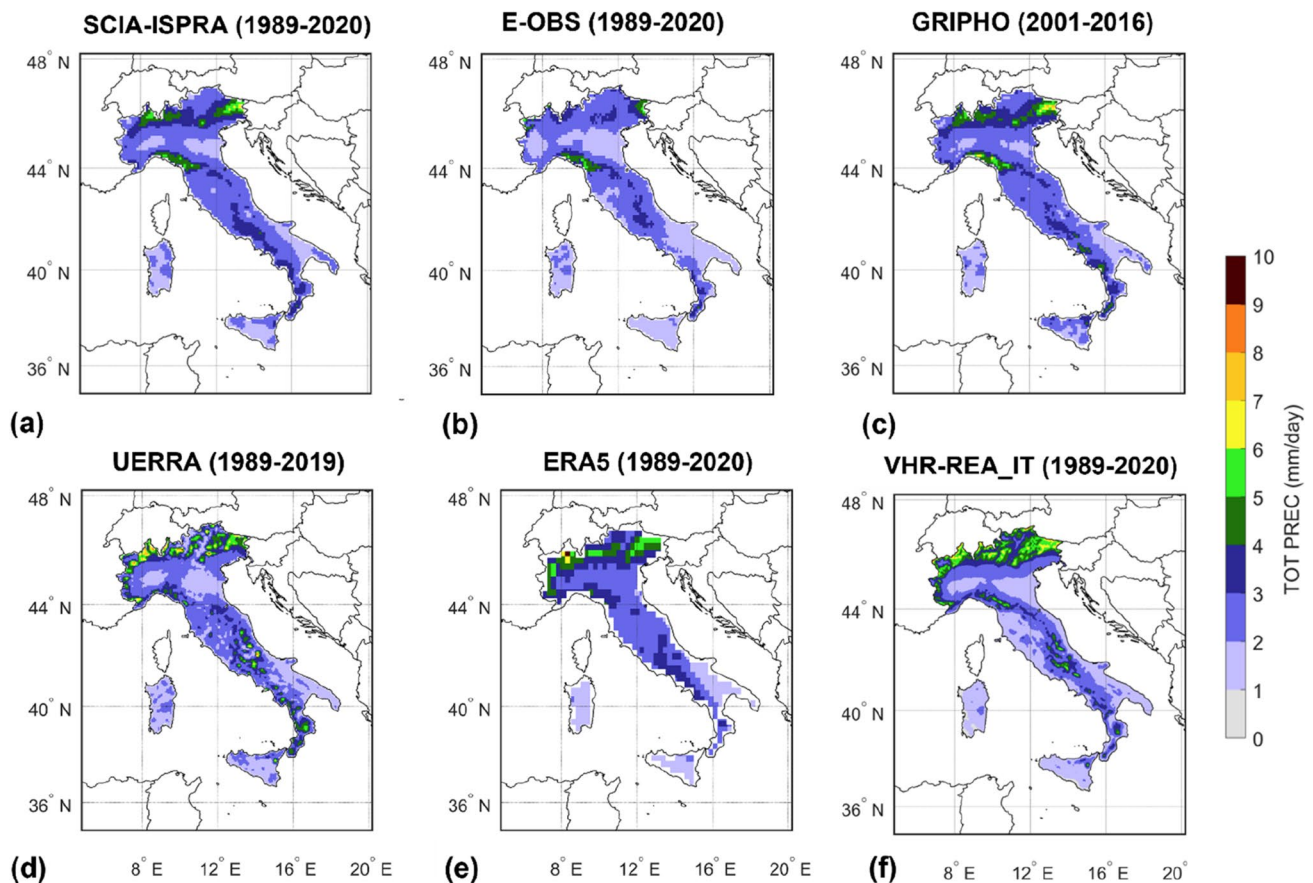


**Fig. 7** Spatial distribution of daily mean precipitation from SCIA-ISPRA (a), E-OBS (b), GRIPHO (c), UERRA (d), ERA5 (e) and VHR-REA\_IT (f). Data for (a), (b), (e) and (f) refer to the period

1989–2020; data for (c) cover the period 2001–2016 and data for (d) cover the period 1989–2019

data from GRIPHO cover 2001–2016 (due to the availability of the dataset).

Although covering different periods, the patterns of precipitation from SCIA-ISPRA and GRIPHO observational datasets (Fig. 7a and c) depict a coherent and uniform spatial distribution. Specifically, mean precipitation is below 4 mm/day, almost the entire peninsula except for the Alpine chain and regions, such as the northern Tyrrhenian coast, featuring more pronounced mean values. Moreover, GRIPHO highlights higher values than SCIA-ISPRA over the southern Mediterranean area (as the Neapolitan coast and coastal areas in the southern Campania region). E-OBS (Fig. 7b) reports lower values than the previous one, especially over the Alps chain and Insular areas. VHR-REA\_IT (Fig. 7f) agrees with observations, SCIA-ISPRA and GRIPHO in particular, reproducing the spatial pattern of precipitation over the whole domain, except over the Alpine area, where the model tends to produce higher daily precipitation values. This behaviour may be partly due to the forcing data (i.e. ERA5 depicted in Fig. 7e) and partly to the snow effect (detailed in §4.2.2). Figure 7e proves that ERA5 tends to

increase precipitation across Italy, especially if compared with E-OBS gridded dataset. The spatial refinement of ERA5 in VHR-REA\_IT at 2.2 km reduces this wet bias. Moreover, the CP-RCMs multi-model study by Ban et al. (2021) also found these overestimations over the Alps, highlighting that daily precipitation has higher values than observations in large-scale precipitation from mid-latitude storms in winter and convective precipitation in summer.

Table 5 reports the yearly and seasonal mean precipitation values derived from SCIA-ISPRA, E-OBS, GRIPHO, UERRA, ERA5 and VHR-REA\_IT. Yearly metrics (i.e. mean values and standard deviations) shown in Table 5 confirm the coherence between observations and the model. The mean value is 2.6 mm/d for SCIA-ISPRA and UERRA and 2.7 mm/d for GRIPHO and ERA5, close to VHR-REA\_IT (2.5 mm/d); instead, it is 2.2 mm/d for E-OBS. In addition, spatial variability is around  $\pm 0.8$  mm/d for all observational datasets, while it is slightly higher for UERRA and ERA5 ( $\pm 1.0$  mm/d) and even higher for VHR-REA\_IT ( $\pm 1.2$  mm/d).

By looking at the seasonal mean precipitation values, the observational references indicate high precipitation

**Table 5** Metrics (mean value and standard deviation) over the whole domain from SCIA-ISPRA, E-OBS, GRIPHO, UERRA, ERA5 and VHR-REA\_IT, related to the spatial precipitation distribution for the period 1989–2020 (the period 2001–2016 is considered for GRIPHO)

	SCIA-ISPRA	E-OBS	GRIPHO	UERRA	ERA5	VHR-REA_IT
YEARLY (mm/d)	2.6 ( $\pm 0.8$ )	2.2 ( $\pm 0.7$ )	2.7 ( $\pm 0.8$ )	2.6 ( $\pm 1.0$ )	2.7 ( $\pm 1.0$ )	2.5 ( $\pm 1.2$ )
SON (mm/d)	3.4 ( $\pm 2.6$ )	3.0 ( $\pm 1.0$ )	3.4 ( $\pm 1.9$ )	3.2 ( $\pm 1.1$ )	3.5 ( $\pm 0.6$ )	3.0 ( $\pm 1.4$ )
DJF (mm/d)	2.7 ( $\pm 2.4$ )	2.3 ( $\pm 0.9$ )	2.8 ( $\pm 2.3$ )	2.2 ( $\pm 0.9$ )	2.5 ( $\pm 0.6$ )	2.3 ( $\pm 0.9$ )
MAM (mm/d)	2.4 ( $\pm 1.3$ )	2.2 ( $\pm 0.7$ )	2.6 ( $\pm 1.2$ )	2.6 ( $\pm 1.0$ )	2.8 ( $\pm 1.0$ )	2.7 ( $\pm 1.3$ )
JJA (mm/d)	1.6 ( $\pm 2.6$ )	1.4 ( $\pm 1.1$ )	1.6 ( $\pm 1.9$ )	2.4 ( $\pm 2.0$ )	2.2 ( $\pm 1.2$ )	2.0 ( $\pm 1.7$ )

Metrics are yearly and seasonally (*SON* September–October–November, *DJF* December–January–February, *MAM* March–April–May, *JJA* June–July–August) reported

**Table 6** DAV metric for total precipitation assessed over Italy (whole domain) and over NUTS1 from VHR-REA\_IT (as high resolution product), SCIA-ISPRA (as observation), UERRA and ERA5 (as low resolution product), respectively

NUTS1	DAV—UERRA (%)	DAV—5 (%)
Italy (whole domain)	7	−5
Northwest	29	33
Northeast	21	4
Central	−21	−32
South	21	3
Insular	−45	−28

in autumn and winter, with values falling in spring and attaining a minimum in summer. In comparison with observations (mainly SCIA-ISPRA and GRIPHO), VHR-REA\_IT reduces precipitation in autumn and winter (3.0 mm/d and 2.3 mm/d, respectively), increasing it in spring (2.7 mm/d) and summer (2.0 mm/d), when convection plays an increased role resulting in higher precipitation value (Ban et al. 2021).

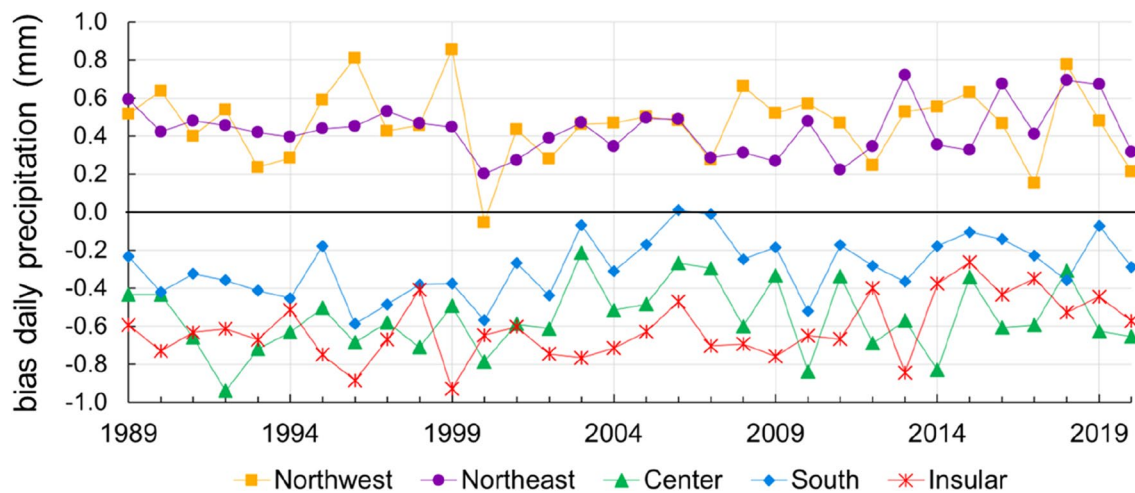
Moreover, the comparison in Figure 7 with reanalysis products highlights that the spatial patterns depicted by UERRA reanalysis slightly overestimate total precipitation in some parts of central and southern Italy if compared with SCIA-ISPRA observations, whereas ERA5 patterns are in good agreement with it. Such qualitative analyses are also confirmed by the DAV metric reported in Table 6, where SCIA-ISPRA is used as the reference. Generally, DAV assessed over all Italy indicates an added value in VHR-REA\_IT of 7% if compared with UERRA reanalysis and a loss of −5% if compared with ERA5. The DAV over NUTS1 indicates that an added value in VHR-REA\_IT is found considering both UERRA and ERA5 over Northern and Southern areas, whereas losses are quantified over Central and Insular areas. These negative DAV values may be related to peculiar circulation patterns occurring, especially along coasts (i.e., where the sea mainly regulates the lateral boundaries, and CCLM is not able to reproduce these dynamics as it is uncoupled from an ocean model; Reder et al. 2022).

Figure 8 draws the yearly evolution of precipitation bias over NUTS1 subdomains. The time-series return a precise spatial repartition of the bias along the Italian peninsula. Specifically, northern Italy (i.e., Northwest NUTS1 and Northeast NUTS1) reveals a slight increase in the simulated total precipitation against observations; such bias is on average 0.5 mm/day with a temporal standard deviation in-between 0.1–0.2 mm/day. On the other hand, the rest of the peninsula points out a slight decrease in the simulated total precipitation; this decrease is limited in the South NUTS1 ( $\approx -0.3$  mm/day) growing in the Central NUTS1 and Insular NUTS1 ( $\approx -0.6$  mm/day). Finally, the temporal standard deviation for these areas is almost the same ( $\approx 0.2$  mm/day).

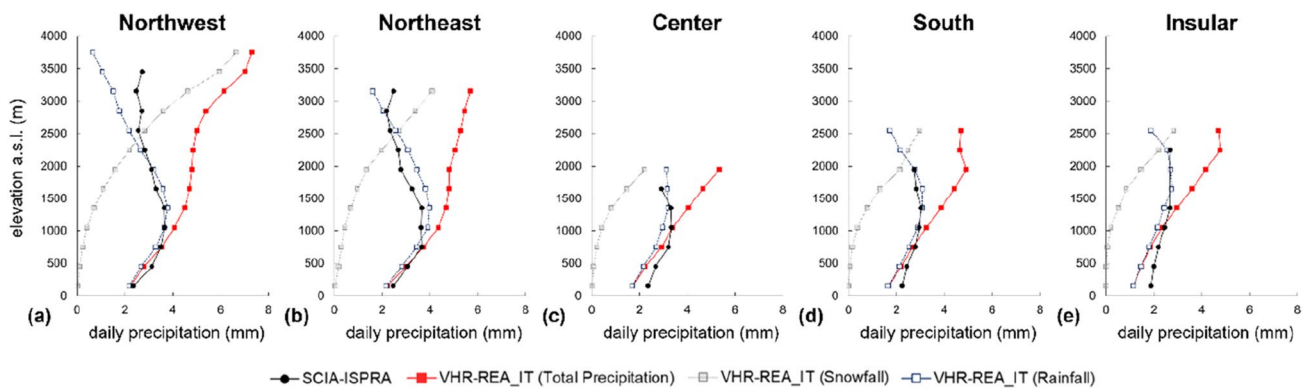
### 3.2.2 Orography effects

Figure 9 displays the altitudinal profiles of mean total precipitation obtained for each NUTS1 (Fig. 9a–e) using SCIA-ISPRA and VHR-REA\_IT. The altitudinal profiles obtained by interpreting the VHR-REA\_IT total precipitation (red line) follow the observation patterns (black line) up to altitudes of around 1000 m and then diverge towards significantly higher values beyond this altitude. Between the bands 1000 m and 4000 m, snow accumulation is likely responsible for the wider spread (Monteiro et al. 2022). Indeed, COSMO-CLM total precipitation includes rainfall and snowfall (i.e., liquid and solid precipitation), while the SCIA-ISPRA observations predominantly incorporate rainfall based on rain gauge measurements. To account for such a difference in the quantification of the total precipitation between the simulation and observation, this work proposes a simplified method relying on temperature data to discern the snowfall component of the modelled total precipitation as the orography increases. Such a method is a modified version of the approach used at the monthly scale in the Thornthwaite water balance model (Thornthwaite and Mather 1955; McCabe and Markstrom 2007) to derive rainfall and snowfall from total precipitation according to mean temperature. It is assumed that the total precipitation is totally snowfall (hence rainfall contribution null) when





**Fig. 8** Evolution of the annual bias of VHR-REA\_IT against SCIA-ISPRA dataset of mean total precipitation over NUTS1



**Fig. 9** Altitudinal profiles of mean total precipitation obtained for each NUTS1 (subplots a-e) using SCIA-ISPRA (black line) and VHR-REA\_IT (red line). Vertical profiles of the detected snowfall (grey line) and rainfall (blue line) contributions from VHR-REA\_IT are also depicted

both maximum and minimum daily 2m-temperatures are lower than zero. At the same time, it is totally rainfall (thus snowfall contribution null) when both are greater than zero. In the case of maximum daily 2m-temperature greater than zero and minimum one lower than zero, a weighted average law for total precipitation - based on mean, maximum and minimum temperatures - is defined to account for both rainfall and snowfall contributions. More details can be found in Appendix, where the procedure is outlined and validated using ERA5 data.

The method provides the snowfall profiles in Fig. 9a-e (grey line) and, consequently, the rainfall ones (blue line) as the difference between the total precipitation and snowfall profiles. The Figure shows snowfall has a negligible contribution for low elevations (less than 1000 m) and increases with altitude, exceeding rainfall contributions for altitude values greater than 2500 m. On the other hand, VHR-REA\_IT rainfall returns altitudinal profiles that match the observations satisfactorily. Specifically, rainfall increases

with altitudes up to 1000 m. It then reverses the altitudinal growth gradient beyond this altitude when part of the precipitation occurs as snowfall. This behaviour also clarifies the precipitation overestimates shown in Fig. 7f over high orography (i.e., the Alps) and is even more evident in Fig. 8 in terms of positive mean annual bias for Northwest Italy and Northeast Italy.

### 3.2.3 Analysis of the summer hourly precipitation

Several studies (Ban et al. 2021; Adinolfi et al. 2021; Kendon et al. 2021; Lucas-Picher et al. 2021) recognised the improved representation of hourly precipitation as an added-value of CP-RCMs. In this view, this Section analyses hourly precipitation features of VHR-REA\_IT, comparing with the driven reanalysis ERA5 and assuming the available hourly dataset (i.e., GRIPHO) as a reference.

Figure 10 shows the aggregated maps for hourly statistics of precipitation intensity (Fig. 10a, d and g), frequency

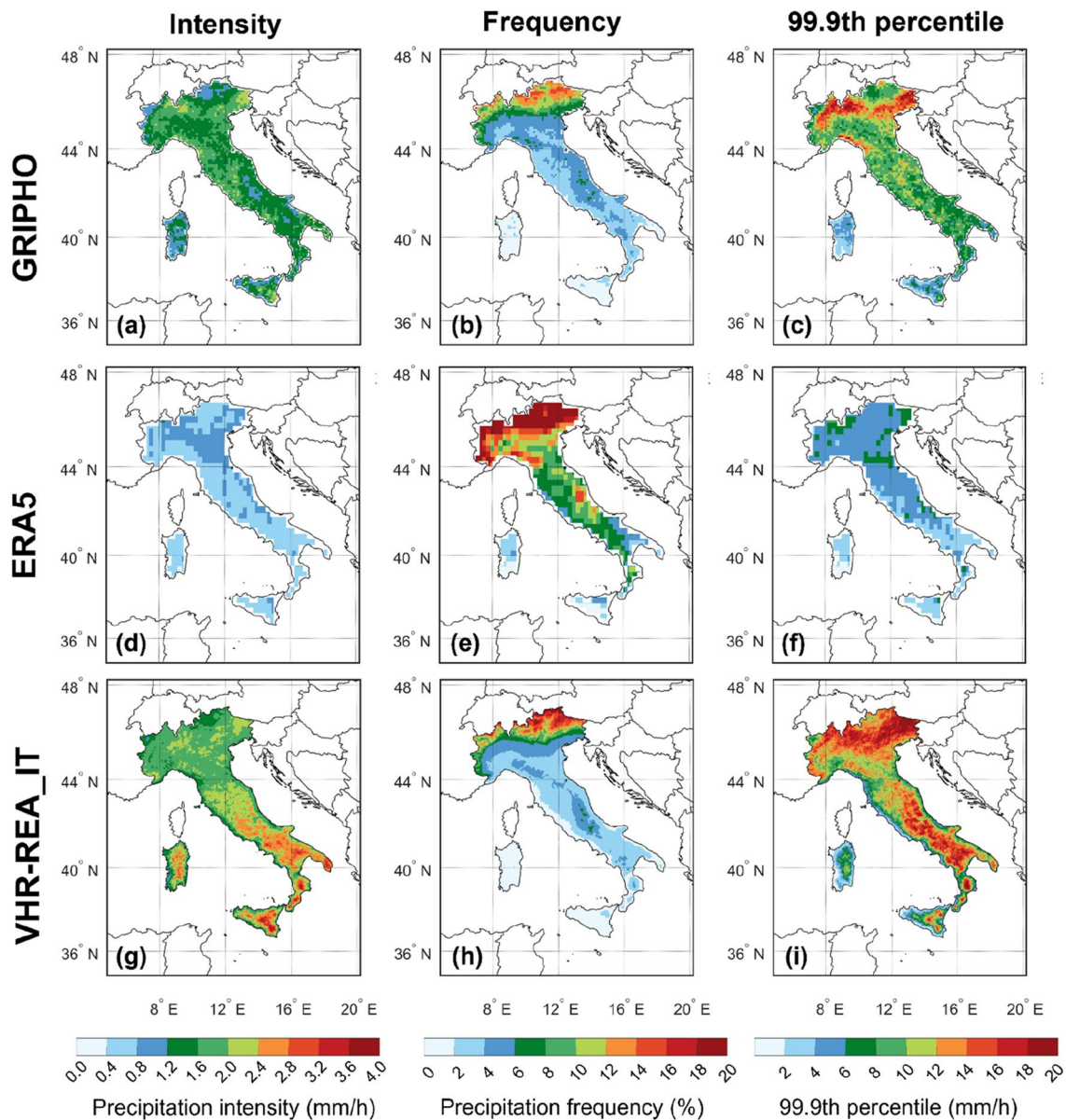


**Fig. 10** Hourly maps for the summer season in the period 2001–2016 in terms of: precipitation intensity retrieved by GRIPHO (a), ERA5 (d) and VHR-REA\_IT (g) datasets; precipitation frequency retrieved by GRIPHO (b), ERA5 (e) and VHR-REA\_IT (h) datasets; heavy

precipitation assessed as the 99.9 percentile of hourly precipitation by GRIPHO (c), ERA5 (f) and by VHR-REA\_IT (i) datasets. Maps are on their native grids

(Fig. 10b, e and h) and 99.9th percentile (Fig. 10c, f and i) for the summer season over 2001–2016 returned by GRIPHO (Fig. 10a–c), ERA5 (Fig. 10d–f) and VHR-REA\_IT (Fig. 10g–i).

VHR-REA\_IT overestimates intensity compared to observations (Fig. 10g against Fig. 10a) over Italy, except for the Alps, where it well-reproduces hourly precipitation intensity. The modelled frequency (Fig. 10h) agrees with the spatial patterns of observations (Fig. 10b), with higher values over the Alps than the rest of the peninsula. The 99.9th percentile of hourly precipitation (representing

heavy precipitation) is fairly modelled by VHR-REA\_IT (Fig. 10i) against observation (Fig. 10c) over the Alps. Still, it is overestimated in the Southern part and the insular areas. Ban et al. (2021) and Adinolfi et al. (2021) returned similar findings by comparing observations with CP-RCMs over a domain covering Northern and Central Italy. Specifically, Ban et al. (2021) argued that overestimations in intensity and 99.9th percentile of hourly precipitation are not necessarily signs of a bad model performance, as a part of these differences can be explained by observational uncertainties due to the sparse observational networks over higher altitudes that

receive more precipitation and interpolation methods used to produce gridded datasets. Moreover, Figure 10 depicts that ERA5 (Fig. 10d-f) strongly overestimates hourly precipitation frequency, whereas it underestimates precipitation intensity and heavy precipitation, in comparison with GRIPHO (Fig. 10a-c) and VHR-REA\_IT (Fig. 10g-i). Reder et al. (2022) returned similar findings analysing precipitation extremes for different cities at CP-RCMs. They stated that each grid point of ERA5 is informative for an area, at least equal to  $31 \times 31 \text{ km}^2$ , and then, for each grid cell, weather variables (i.e., for precipitation, Reder and Rianna 2021) can be affected in their magnitude by an averaging effect which produces a smoothing, especially for hourly extreme precipitation values. Such a smoothing effect decreases with spatial resolution enhancement. This aspect returns evidence of benefits induced by the convection-permitting model in representing hourly precipitation features.

In addition, heavy precipitation is statistically analysed as whiskers box plots in Figure 11 at the NUTS1 level. It is worth noting that VHR-REA\_IT data is remapped over the GRIPHO grid, so the remapping procedure could induce artificial errors due to smoothing or representativity errors. The box plots from GRIPHO return Northwest and Northeast median values of around 11 mm/h. VHR-REA\_IT represents with a good agreement the Northwest and overestimates Northeast NUTS1 with a shift of around 3 mm/h. The median values in the Insular area are close to 5 mm/h for both observation and model. The main differences between model and observation occur over the South area, in representing the median and 95th percentile, and in the 5th percentile for the Central NUTS1. To sum up, VHR-REA\_IT

increases the distribution of heavy hourly precipitation in median and percentiles.

The findings highlight that the spatial refinement of VHR-REA\_IT is able to reproduce the hourly precipitation features more in the complex orographic areas (i.e., Northwest and Northeast NUTS1) than in other territories (i.e. South, Central and Insular NUTS1). They also agree with previous studies (Berthou et al. 2020; Adinolfi et al. 2021) and multi-model ensemble (Ban et al. 2021) at the convection-permitting scale over the Alpine area.

Moreover, diurnal cycles of precipitation intensity and wet-hour frequency are averaged in summer (2001–2016) over NUTS1, as shown in Figures 12 and 13, respectively. The km-scale patterns improve the representation of diurnal cycles both for precipitation intensity and wet-hour frequency. For intensity (Fig. 12), the values and timing of GRIPHO over all NUTS1 are much better captured by VHR-REA\_IT than ERA5. The latter systematically underestimates the hourly intensity. When looking into the diurnal cycle of wet-hour frequency (Fig. 13), VHR-REA\_IT figures out a good match with GRIPHO, especially over Northeast and Northwest NUTS1. ERA5 systematically overestimates the wet-hour frequency over all NUTS1. The diurnal cycles of summer intensity and wet-hour frequency reveal that VHR-REA\_IT shows superior performance to the coarse resolution ERA5 Reanalyses. It is a further confirmation that the longstanding problem of incorrect timing with too frequent and too weak precipitation is greatly improved by switching on the parameterisation of convection (Ban et al. 2021). However, some deficiencies persist in the CP-RCMs modelling system that need to be addressed in the future.

**Hourly Heavy Precipitation (99.9th percentile) over summer period (JJA | 2001–2016)**

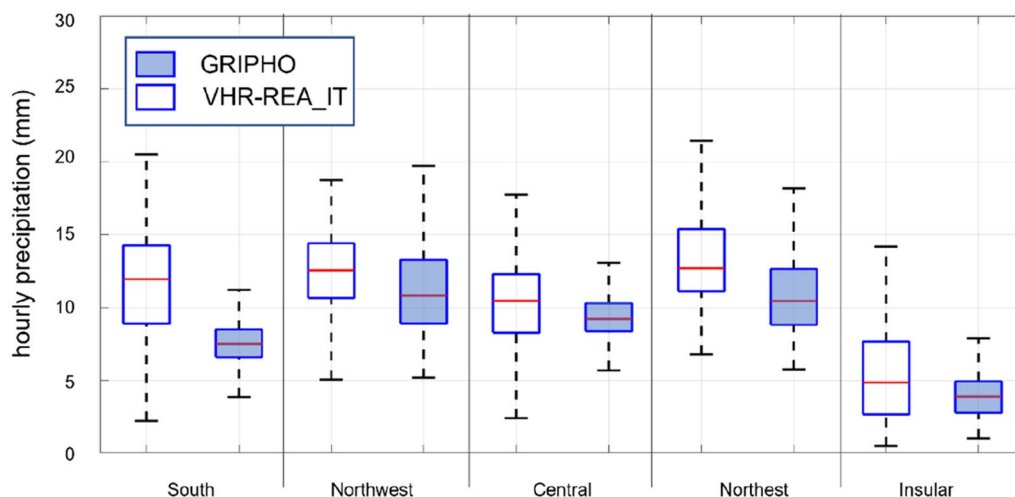


**Fig. 11** Box plots over NUTS1 for the period 2001–2016 in terms of summer heavy precipitation assessed as the 99.9 percentile of hourly precipitation from GRIPHO and VHR-REA\_IT

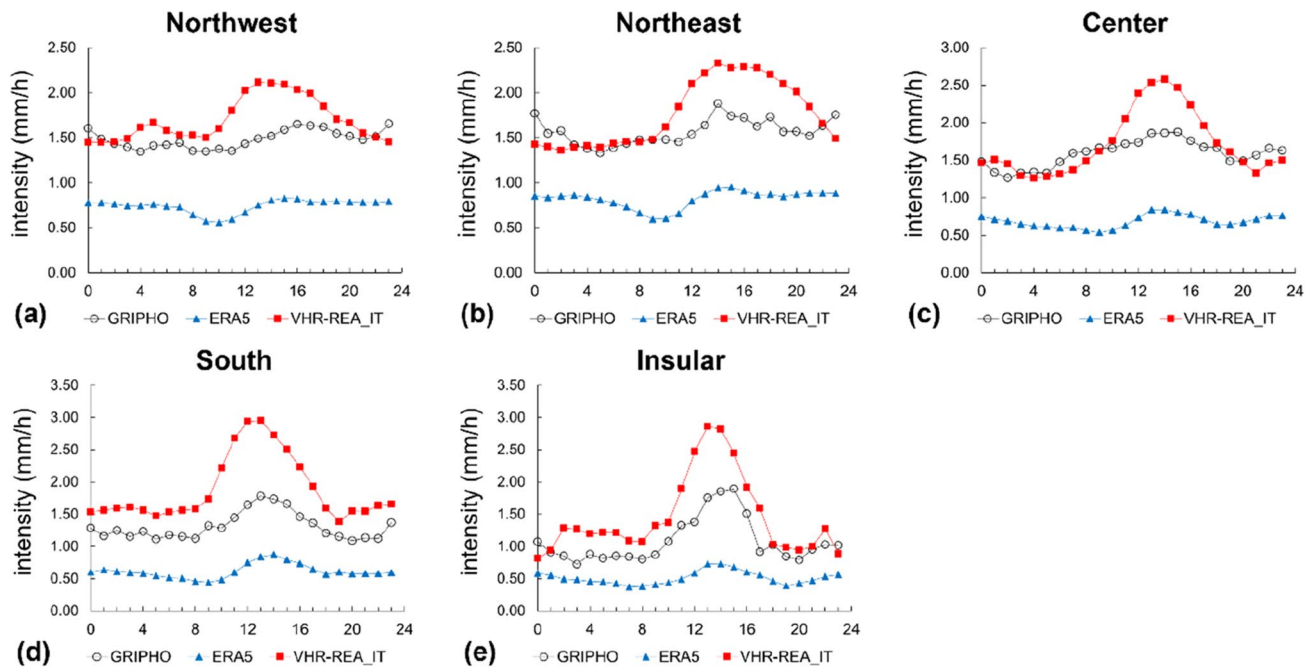


**Fig. 12** Diurnal cycle of precipitation intensity averaged over NUTS1 for the period 2001–2016 (in summer) from GRIPHO, ERA5 and VHR-REA\_IT

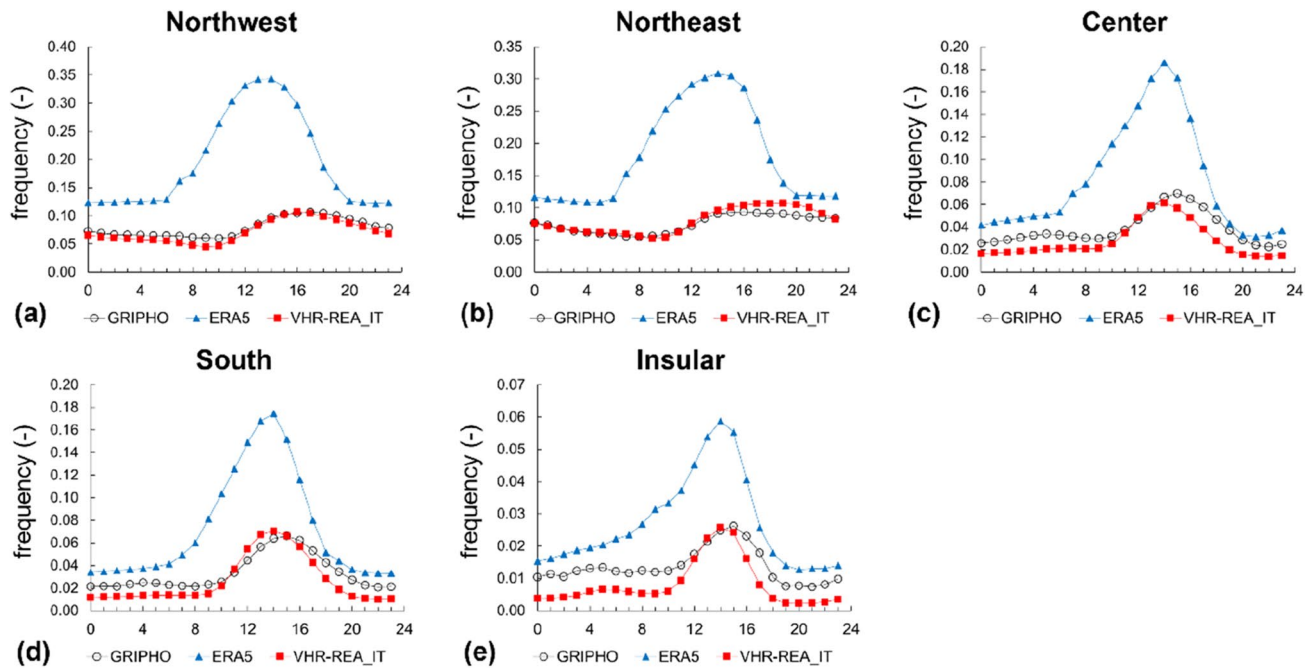


**Fig. 13** Diurnal cycle of wet-hour frequency averaged over NUTS1 for the period 2001–2016 (in summer) from GRIPHO, ERA5 and VHR-REA\_IT



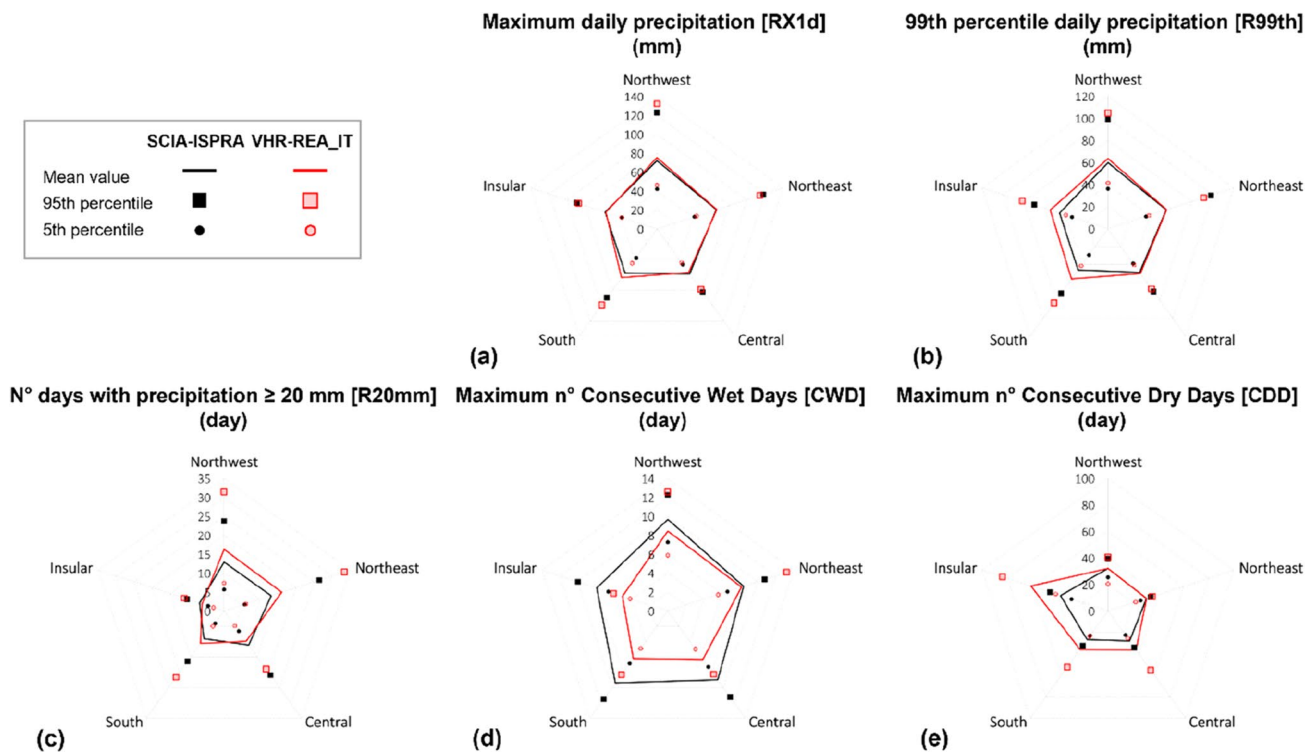


**Fig. 14** Radar chart for precipitation-related ETCCDI climate indicators for 1989–2020 for each NUTS1. The plots provide mean (continuous line), 5th percentile (filled circle) and 95th percentile (filled square) values of indicators allowing the comparison between the VHR-REA\_IT (red lines and fills) and SCIA-ISPRA (black lines and

fills) datasets. The retrieved climate indicators are: **a** maximum daily precipitation—RX1d, **b** 99th percentile daily precipitation—R99th, **c** N° days with precipitation  $\geq 20$  mm—R20mm, **d** Maximum n° Consecutive Wet Days—CWD and **e** Maximum n° Consecutive Dry Days—CDD

**Table 7** VHR-REA\_IT minus SCIA-ISPRA mean values of the selected climate indicators for precipitation over NUTS1

	Northwest	Northeast	Central	South	Insular
RX1d (%)	4%	0%	−3%	12%	−2%
R99th (%)	7%	0%	2%	22%	20%
R20mm (%)	23%	23%	−9%	22%	−14%
CWD (%)	−20%	0%	−33%	−33%	−38%
CDD (%)	0%	0%	29%	33%	61%

Values are reported as percentage bias (model-observation)/observation

### 3.2.4 Extreme precipitation indices

Figure 14 displays the precipitation-based ETCCDI climate indicators, introduced in §2 and listed in Table 1. Data are represented for 1989–2020 using the radar chart for each NUTS1. The plots provide mean (continuous line), 5th percentile (filled circle) and 95th percentile (filled square) values of indicators allowing the comparison between the VHR-REA\_IT and SCIA-ISPRA datasets. The values are also provided in Table 7 as mean value differences between VHR-REA\_IT and SCIA-ISPRA.

VHR-REA\_IT fairly and uniformly detects the observed distribution of RX1d (Fig. 14a) and R99th (Fig. 14b) as for mean as for percentiles, although for R99th slight overestimations over South and Insular areas occur. Moreover, the R20mm (Fig. 14c) distribution is quite well represented by VHR-REA\_IT compared with observations over the Insular, Southern and Central areas, and some overestimations are represented over the Northeast and Northwest areas. On the other hand, for CWD (Fig. 14d) and CDD (Fig. 14e), simulation differs from observations. Specifically, VHR-REA\_IT returns a shifted distribution for CWD compared to observations over all NUTS1, but Northeast. It means that the simulation underestimates both mean and percentile values. Consequently, VHR-REA\_IT generally overestimates CDD against observations. This is mainly evident in the Insular, South and Central areas.

To sum up, maximum daily precipitation and 99th percentile of daily precipitation are uniform and well reproduced by VHR-REA\_IT. The same is for the number of days with precipitation  $\geq 20$  mm. A response dependent on the region, especially in topographically complex areas, is performed by the maximum number of consecutive wet and dry days, highlighting a better performance of VHR-REA\_IT in

mountainous Northern NUTS1 and differences in the South, Central and Insular NUTS1 with non-uniform radar plot.

Zollo et al. (2016) performed a similar analysis for precipitation extremes over Italy (in particular in four regions, i.e., Veneto, Tuscany, Calabria, and Sardinia, which can be assumed as indicative of Northeast, Central, Southern and Insular NUTS1). They exploited a simulation performed with the RCM COSMO-CLM at a horizontal resolution of ~ 8 km driven by the ERA-Interim reanalysis (Dee et al. 2011). In general, the authors highlighted a general tendency of the model towards underestimation, except for the number of CDD. Compared with Zollo et al. (2016), this work improves the representation of RX1d, R99th, and R20mm by reducing the bias between the model and observations. However, some deficiencies still need improvement in representing the frequency of wet/dry days. As done in this work, adopting a threshold of 1 mm to discriminate between wet and dry days may partly mitigate such an issue. Although CP-RCMs largely improve the tendency (Figs. 12, 13) to trigger excessively frequent and weak precipitation events (the so-called “drizzle effect” as in Gutowski et al., 2003) in the coarser resolution models (Pichelli et al. 2021), CP-RCMs present drier conditions than the corresponding RCMs (Sangelantoni et al. 2023), and it is not possible to fully disentangle the role of resolution increase against the role of improved physics, which are inextricably linked. Both the land-atmosphere interactions and microphysical parameterisations could be regarded as the key factors behind these modifications introduced by the km-scale modelling (Milovac et al. 2016). For example, large uncertainty affects the representation of the soil moisture-precipitation feedback, which remains a challenge (Yang et al. 2018; Kendon et al. 2021; Leutwyler et al. 2013).

## 4 Conclusions

The paper analysed VHR-REA\_IT, a dynamical downscaling of ERA5 recently performed over Italy through the COSMO-CLM model at a convection-permitting scale, turning on the urban scheme TERRA-URB. The atmospheric variables coming from VHR-REA\_IT (introduced in Raffa et al. 2021a) provide accurate information on the actual local synoptic weather situation. Although Raffa et al. (2021a) is a data descriptor paper, it presented some preliminary and seasonal analyses (i.e. spatial patterns and statistics) with respect to E-OBS and ERA5. The current study integrated Raffa et al. (2021a) analyses with further statistical evaluations, metrics and reference products, focusing on 2m temperature and precipitation, assumed as the two variables commonly adopted in climate assessments. The capability of VHR-REA\_IT in realistically representing the climatology over the whole domain and subdomains (NUTS1) as well as

capturing specific features, has been tested. The main results of the study are summarised in the following:

1. The first achievement is the assessment of climate data over Italy with increased space (2.2 km) and time (1 h) resolutions for a 30-year long period (1989–2020). Such continuous reanalysis-driven downscaling has the advantage of overcoming the common time-slice approach (i.e. based on 10-year period of simulation) limitations, usually used due to the computational burden, therefore it goes some steps forward compared with the current state-of-the-art. Indeed, VHR-REA\_IT allows computing robust climate statistics based on enough long period of simulation (i.e. 30 years) with a proper evaluation of extremes, reducing potential uncertainties due to natural climate variability. Of course, the uncertainties due to internal variability still persist since one single model was used to run the dynamical downscaling.
2. The second achievement relies on the challenging setup defined to run the reanalysis-driven simulation, bringing the potential of convection-permitting models and urban parameterisation. The dynamical downscaling setup, associated with a proper methodology for the evaluation, allows us to draw a clear picture of the current climate over Italy for mean values and extremes, thanks to the very high spatial resolution implemented. The capability of VHR-REA\_IT in reproducing observational spatial patterns of daily mean temperature and precipitation from several observational datasets is demonstrated. Encouraging values of the metric for the assessment of the added value (i.e. DAV) are in favour of VHR-REA\_IT. Moreover, it reproduces observational spatial patterns of daily mean temperature in good agreement (see Fig. 2), especially over the mountainous areas. On the other hand, it returns a warm temperature bias over flat terrain mainly due to the soil moisture-precipitation feedback modification acting when an explicit treatment of deep-convection processes is turned on (Hohenegger et al. 2009; Taylor et al. 2013). This issue is a well-known and an independent-model behaviour investigated in CP-RCMs multi-model studies (Sangelantoni et al. 2023; Soares et al. 2022), revealing the need to assess the applicability of parameterisations, designed for coarser resolutions to kilometre scales (as the land–atmosphere interactions and microphysical parameterisation). Furthermore, VHR-REA\_IT consistently highlights the ability of urban parameterisation to represent urban heat as the local detection of minimum temperature during summer. This result is particularly evident in the case of Milan city (see Fig. 5). Such a capacity makes the urban parameterization used for the dynamical downscaling VHR-REA\_IT a powerful tool to improve regional climate models, support local adap-

tation actions and impact studies in the urban environment.

The spatial distribution of daily mean precipitation reveals that VHR-REA\_IT accurately represents past and current precipitation patterns and agrees with observations over the whole domain, except the Alpine area, where the model returns higher values. It could be possibly due to the forcing data and partly to the snow effect. An interesting - although simplified - approach is proposed to account for the snowfall component of the total precipitation at high altitudes: VHR-REA\_IT rainfall returns vertical profiles that match the observations satisfactorily and increase with altitudes up to 1000 m. Beyond this altitude, part of the precipitation occurs as snowfall. This behaviour also clarifies the precipitation overestimates over the Northern part of the peninsula. Moreover, hourly analyses show that the modelled intensity of wet hours in summer and the heavy precipitation events, in terms of the 99.9th percentile, are overestimated if compared with reference products, especially over the South part of the peninsula. In contrast, over the Alps, the agreement is satisfactory. The modelled frequency of wet hours in summer agrees with observations. Both simulation and observations depict higher values over the Alps than in the remaining part of the peninsula. The ability of VHR-REA\_IT is mainly in the representation of hourly intensity, frequency and heavy precipitation if compared with ERA5 patterns (see Figure 10), clearly showing the benefits of explicitly-solved convection. Such capability is also proved by the diurnal cycles (Figs. 12, 13), where ERA5 systematically underestimates the hourly intensity and overestimates the wet-hour frequency over all NUTS1, but VHR-REA\_IT figures out a good match with GRIPHO in the representation of values and timing. Therefore, this study corroborates the advantages of the use of CP-RCMs, as Prein et al. (2013), Kendon et al. (2021), Adinolfi et al. (2021) and multi-model studies (Ban et al. 2021; Müller et al. 2022).

3. The third achievement consists in assessing extreme events on a detailed scale through climate indicators. It is worth noting that climate indicators are useful tools for the assessment of extreme events in terms of magnitude, occurrence and impacts (Kjellström et al. 2010; Devkota and Bhattarai 2018). For instance, the number of consecutive dry days constitutes essential information in drought studies. At the same time, the maximum daily precipitation may provide information supporting, as an example, flooding and landslides studies. Finally, the number of tropical nights is closely connected to the occurrence of heatwaves. The evaluation highlights that indicators based on the percentiles of 2 m temperature (TX90th and TN10th, respectively) are uniform and well reproduced by VHR-REA\_IT as well as the frequency

indicators such as summer days and tropical nights (SU and TR, respectively). A response from both observations and model dependent on the region is performed by frost days (FD), magnifying differences between Northern and Southern areas. The indicators based on maximum and percentiles of precipitation (RX1d and R99th, respectively) are uniform and well reproduced by VHR-REA\_IT. A response dependent on the region is performed by the maximum number of consecutive wet and dry days, highlighting a better performance of VHR-REA\_IT in mountainous Northern NUTS1 and discrepancies in the South, Central and Insular NUTS1. The climate indicators recognise the occurrence of extreme events at a detailed scale, becoming a relevant tool in turning climate data into information.

In recent years, assessing the added value of CP-RCMs in the representation of precipitation patterns, compared to coarser resolution RCMs, has been one of the main topics of climate studies, as evidenced by recent initiatives such as the CORDEX FPS-CONV. This paper aimed to support the research activities with this goal, proving the limitations and abilities of VHR-REA\_IT in representing past and current 2m temperature and precipitation patterns over complex contexts. This aim was addressed by analysing a 30-years long simulation against ERA5 and other reference products (i.e. observational gridded datasets and reanalyses). The main impact of this study is mainly intended for research purposes in the field of climate studies. Thus, the findings cannot properly support decision-making and adaptation assessments, as results are derived from one-single dynamical downscaling and affected by model uncertainties. To cope with this issue, multi-model ensembles are necessary to span the full range of uncertainties (Fosser et al. 2015; Ban et al. 2021). However, a multi-model long-time CP-RCMs ensemble derived from a coordinated initiative over Italy is currently unavailable. The key scientific results presented in this paper highlighted the benefits and limitations of CP-RCMs, contributing further to the current state-of-the-art on this topic. In particular, benefits are gained in mountainous areas where the CP-RCMs are proven to fairly represent the 2m temperature and hourly precipitation features. Over urban contexts, the here adopted urban parameterisation is proved to simulate city heat detection. Losses in performances occur over coastal and flat areas of the Italian peninsula, where the performance of the CP-RCM does not seem to be satisfactory. The presented potentialities and limitations are affected by the peculiarities of the Italian peninsula, characterised by orographic features, terrain close to the coast and complex urban development.

Moreover, the proposed findings would support the scientific activities in the climate community to find a proper trade-off between the improvements and obstacles

of running CP-RCMs. On the one hand, the fine spatial and temporal scales and the demonstrated benefits make CP-RCMs attractive tools to represent climate features. They open up a wide field of research applications related to the impacts of climate change. On the other hand, the limitations of the CP-RCMs over some territories raise the question of whether the additional computational cost required by CP-RCMs is justified. Specifically, VHR\_REA-IT required 2160 cores and employed about 61 h to perform a 1-year simulation (Raffa et al. 2021a), producing a large amount of data (around 8 TB of output data and around 70 TB of forcing data in terms of 3-dimensional boundary data needed for the downscaling).

As future developments, the role of the data assimilation procedure on downscaling activities (not included in VHR-REA-IT) could be addressed by comparing it with regional reanalyses over Italy driven by ERA5 (Bonanno et al. 2019, Capecchi et al. 2022, Giordani et al. 2023 and Cerenzia et al. 2022).

## Appendix

### Approach to discern rainfall and snowfall components of total precipitation

The annex describes the approach adopted to account, in the total precipitation (tp) returned by the climate model, of the rainfall (rf) and snowfall (sf) components. This approach employs 2 m air temperature and in particular the maximum (tasmax), minimum (tasmin) and mean

(tas) values, as discriminating variables. Specifically, for a generic day  $i$ :

- (1) when  $\text{tasmax}(i) < 0$  and consequently also  $\text{tasmin}(i) < 0$ , it is assumed that all precipitation occurs in the form of snowfall and therefore:

$$\begin{aligned} \text{sf}(i) &= \text{tp}(i) \\ \text{rf}(i) &= 0 \end{aligned} \quad (\text{A.1})$$

- (2) otherwise when  $\text{tasmin}(i) > 0$  and consequently also  $\text{tasmax}(i) > 0$ , it is assumed that all precipitation occurs in the form of rainfall and therefore:

$$\begin{aligned} \text{sf}(i) &= 0 \\ \text{rf}(i) &= \text{tp}(i) \end{aligned} \quad (\text{A.2})$$

- (3) finally, during the intermediate condition characterised by  $\text{tasmax}(i) > 0$  and  $\text{tasmin}(i) < 0$ , it is assumed that precipitation can occur in a day either in the form of snowfall or rainfall. To discern between snowfall and rainfall, a proportionality coefficient  $k$  is included:

$$k = [\text{tas}(i) - \text{tasmin}(i)] / [\text{tasmax}(i) - \text{tasmin}(i)] \quad (\text{A.3})$$

Specifically,  $k=0$  means that  $\text{tas}(i) = \text{tasmin}(i)$  that is total precipitation totally equal to snowfall; otherwise  $k=1$  means that  $\text{tas}(i) = \text{tasmax}(i)$  that is total precipitation totally equal to rainfall; finally,  $k=0.5$  means that  $\text{tas}(i) = 0.5[\text{tasmax}(i) + \text{tasmin}(i)]$  that is half part of total precipitation is equal to snowfall and half part to rainfall.

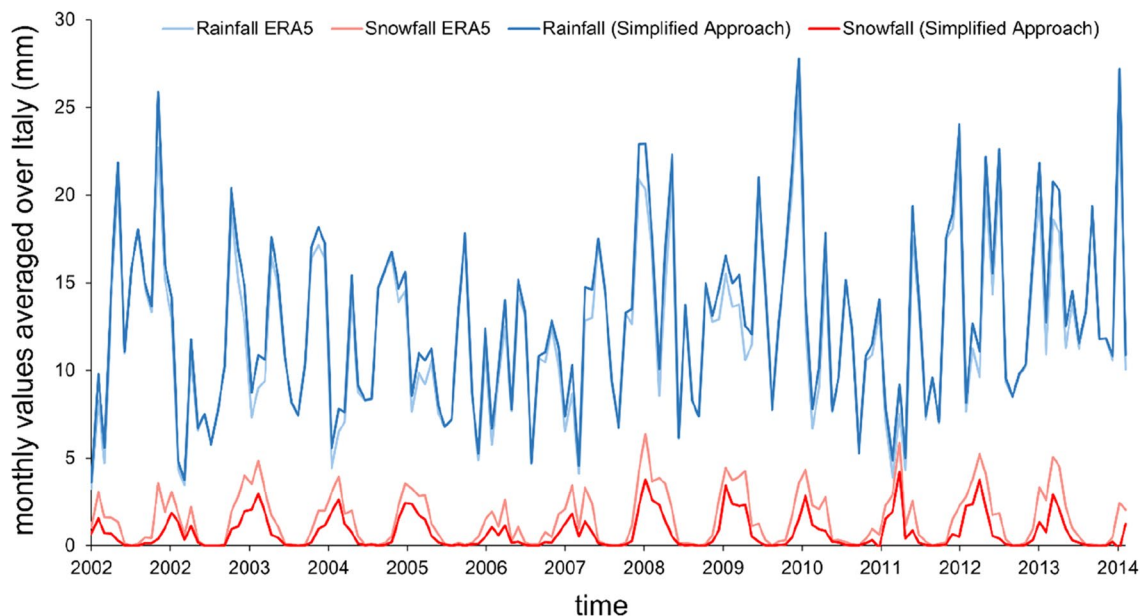


**Fig. 15** Monthly evolution of rainfall and snowfall as returned by ERA5 and as estimated using the simplified approach. Data refer to 2002–2014



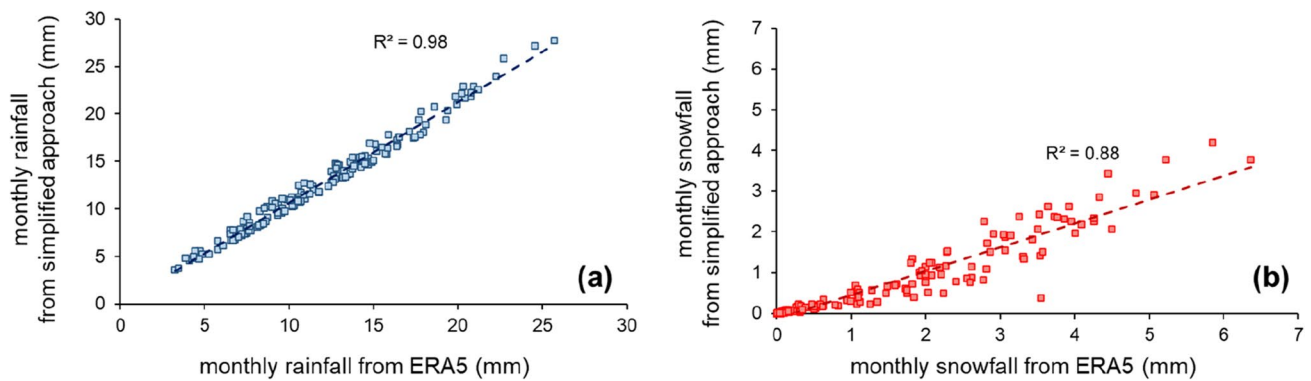


**Fig. 16** Pairs of monthly values of rainfall (a) and snowfall (b) as returned by ERA5 and as estimated using the simplified approach. Data refer to 2002–2014

Given the coefficient  $k$ , it is possible to determine:

$$\begin{aligned} sf(i) &= tp(i) - rf(i) \\ rf(i) &= k \times tp(i) \end{aligned} \quad (A.4)$$

The introduced approach is validated considering the snowfall data from the ERA5 reanalysis. For this purpose, 13 years of data (i.e., 2002–2014) have been processed. The validation consists of comparing the snowfall returned by the approach with the snowfall returned by ERA5. The analysis has been performed on the entire Italian domain and the results are shown both as monthly time series (Fig. 15 in Appendix) and scatter plots (Fig. 16 in Appendix).

The evolutions obtained with the simplified approach agree with those returned in output by ERA5. In particular, the rainfall variable shows a coefficient of determination  $R^2$  practically close to unity (0.98). At the same time, very satisfactory performances are returned by the snowfall variable, characterised by a coefficient of determination  $R^2$  of approximately 0.88. This simple comparison proves the validity of the simplified approach adopted, which makes it possible to easily discriminate the rainfall and snowfall components from the total precipitation on a daily scale.

**Acknowledgements** The authors sincerely thank the HIGHLANDER (HIGH performance computing to support smart LAND sERVICES) project (<https://highlanderproject.eu/>), which is funded by the Connecting European Facility (CEF) Telecommunications sector under agreement number INEA/CEF/ICT/A2018/1815462. The experiments have been performed using the COSMO model in Climate Mode (COSMO-CLM). COSMO-CLM is the community model of the German regional climate research jointly further developed by the CLM-Community. The authors acknowledge the members of the community for their common efforts to develop the model and to find the right setups. The authors would like to thank Emanuela Pichelli and Erika Coppola from UNESCO ICTP for allowing access to the Italian database of precipitation GRIPHO and the WCRP-CORDEX-FPS on Convective phenomena at high resolution over Europe and the Mediterranean. Acknowledgment is also made for the Italian Institute for Environmental Protection and Research (ISPRA) that made the

SCIA-ISPRA dataset freely available by through public web access ([scia.isprambiente.it](https://scia.isprambiente.it/)), exploiting the national system for climate data collection, processing and dissemination. UERRA and ERA5 have been obtained using Copernicus Climate Change Service Information and downloaded from the C3S CDS. Finally, we acknowledge the E-OBS dataset and the data providers in the ECA&D project (<https://www.ecad.eu>). The authors are also grateful to the anonymous reviews for their comments and suggestions, which enabled them to improve the manuscript.

**Authors contribution** All authors contributed to the study conception and design. Conceptualization and methodology, AR, MA, MR and PM; software, MR; validation, MR, MA and AR; formal analysis, MR, AR; investigation, PM and AR; data curation, MR, MA and AR; writing—original draft preparation, MA; writing review and editing, MA, AR and PM; visualization, MR; supervision, PM All authors have read and agreed to the published version of the manuscript.

**Funding** The authors declare that no funds, grants, or other support were received during the preparation of this manuscript.

**Data availability** The VHR-REA\_IT dataset generated during and analysed during the current study is available through the CMCC Data Delivery System ([https://doi.org/10.25424/cmcc/era5-2km\\_italy](https://doi.org/10.25424/cmcc/era5-2km_italy)) and detailed in Raffa et al. 2021a.

## Declarations

**Conflict of interest** The authors have no relevant financial or non-financial interests to disclose.

**Open Access** This article is licensed under a Creative Commons Attribution 4.0 International License, which permits use, sharing, adaptation, distribution and reproduction in any medium or format, as long as you give appropriate credit to the original author(s) and the source, provide a link to the Creative Commons licence, and indicate if changes were made. The images or other third party material in this article are included in the article's Creative Commons licence, unless indicated otherwise in a credit line to the material. If material is not included in the article's Creative Commons licence and your intended use is not permitted by statutory regulation or exceeds the permitted use, you will need to obtain permission directly from the copyright holder. To view a copy of this licence, visit <http://creativecommons.org/licenses/by/4.0/>.

## References

- Adinolfi M, Raffa M, Reder A, Mercogliano P (2021) Evaluation and expected changes of summer precipitation at convection permitting scale with COSMO-CLM over alpine space. *Atmosphere* 12:54. <https://doi.org/10.3390/atmos12010054>
- Allen, R.G., Pereira, L.S., Raes, D., Smith, M. (1998). *FAO Irrigation and Drainage. Paper No. 56: Crop Evapotranspiration (Guidelines for Computing Crop Water Requirements)*. ISBN 92–5–104219–5.
- Amponsah W, Ayrat P A, Boudevillain B, Bouvier C, Braud I, Brunet P, ..., Borga M (2018) Integrated high-resolution dataset of high-intensity European and Mediterranean flash floods. *Earth System Science Data* 10, 1783–1794
- Baldauf M, Seifert A, Förstner J, Majewski D, Raschendorfer M, Reinhardt T (2011) Operational convective-scale numerical weather prediction with the COSMO model: description and sensitivities. *Mon Weather Rev* 139:3887–3905. <https://doi.org/10.1175/MWR-D-10-05013.1>
- Ban N, Caillaud C, Coppola E, Pichelli E, Sobolowski S, Adinolfi M, ..., Zander MJ (2021) The first multi-model ensemble of regional climate simulations at kilometer-scale resolution, part I: evaluation of precipitation. *Climate Dynamics*, 57, 275–302, doi:<https://doi.org/10.1007/s00382-021-05708-w>
- Bartholomé E, Belward AS (2005) GLC2000: A new approach to global land cover mapping from Earth observation data. *Int J Remote Sens* 26:1959–1977. <https://doi.org/10.1080/01431160412331291297>
- Bazile E, Abida R, Verelle A, Le Moigne P, Szczypta C (2017) *MESCAN-SURFEX Surface Analysis. Deliverable D2.8 of the UERRA Project 2017.*
- Berthou S, Kendon EJ, Chan SC, Ban N, Leutwyler D, Schär C, Fossler G (2020) Pan-european climate at convection-permitting scale: A model intercomparison study. *Clim Dyn* 55:35–59. <https://doi.org/10.1007/s00382-018-4114-6>
- Bonanno R, Lacavalla M, Sperati S (2019) A new high-resolution Meteorological Reanalysis Italian Dataset: MERIDA. *Q J R Meteorol Soc* 145(721):1756–1779. <https://doi.org/10.1002/qj.3530>
- Bucchignani E, Montesarchio M, Zollo AL, Mercogliano P (2016) High-resolution climate simulations with COSMO-CLM over Italy: performance evaluation and climate projections for the 21st century. *Int J Climatol* 36:735–756. <https://doi.org/10.1002/joc.4379>
- Cacciamani C, Battaglia F, Patruno P, Pomi L, Selvini A, Tibaldi S (1995) A climatological study of thunderstorm activity in the Po Valley. *Theoret Appl Climatol* 50:185–203. <https://doi.org/10.1007/BF00866116>
- Capecchi V, Pasi F, Gozzini B et al (2022) A convection-permitting and limited-area model hindcast driven by ERA5 data: precipitation performances in Italy. *Clim Dyn*. <https://doi.org/10.1007/s00382-022-06633-2>
- Cardoso, R. M., Soares, P. M (2022) Is there added value in the EURO-CORDEX hindcast temperature simulations? Assessing the added value using climate distributions in Europe. *International Journal of Climatology*, doi:<https://doi.org/10.1002/joc.7472>
- Caretto JAM, Soares PMM, Cardoso RM, Herrera S, Gutiérrez JM (2022) Added value of EURO-CORDEX high-resolution downscaling over the Iberian Peninsula revisited—Part 2: Max and min temperature. *Geoscientific Model Development* 15(6):2653–2671. <https://doi.org/10.5194/gmd-15-2653-2022>
- Cavcar M (2000) *The international standard atmosphere (ISA)*. Anadolu University, Turkey 30(9):1–6
- Cerenzia I. M. L., Giordani A, Paccagnella T, Montani A. (2022). Towards a convection-permitting regional reanalysis over the Italian domain. *Meteorological Applications*, 29(5), e2092, doi:<https://doi.org/10.1002/met.2092>
- Coppola E, Sobolowski S, Pichelli E, Raffaele F, Ahrens B, Anders I, Ban N, Bastin S, Belda M, Belušić, D., et al (2020) A first-of-its-kind multi-model convection permitting ensemble for investigating convective phenomena over Europe and the Mediterranean. *Clim Dyn* 55:3–34. <https://doi.org/10.1007/s00382-018-4521-8>
- Cornes RC, Van Der Schrier G, Besselaar EVD, Jones PD (2018) An Ensemble Version of the E-OBS Temperature and Precipitation Data Sets. *J Geophys Res Atmos* 123:9391–9409. <https://doi.org/10.1029/2017JD028200>
- Dee D et al (2011) The era-interim reanalysis: configuration and performance of the data assimilation system. *Q J R Meteorol Soc* 137:553–597. <https://doi.org/10.1002/qj.828>
- Desiato F, Fioravanti G, Frascchetti P, Perconti W, Toreti A (2011) Climate indicators for Italy: calculation and dissemination. *Adv Sci Res* 6:147–150. <https://doi.org/10.5194/asr-6-147-2011>
- Devkota, R. P., & Bhattarai, U. (2018). Assessment of climate change impact on floods from a techno-social perspective. *Journal of Flood Risk Management*, 11, S186–S196, doi: <https://doi.org/10.1111/jfr3.12192>
- Doms, G., Forstner, J., Heise, E., Herzog, H.J., Mironov, D., Raschendorfer, T., Reinhardt, T., Ritter, B., Schrodin, R., Schulz, J.P., Vogel, G. (2021) A Description of the Non-Hydrostatic Regional COSMO Model. Part-II: Physical Parameterization. Available online: <http://www.cosmo-model.org/content/model/documentation/core/default.htm>
- Doms G, Baldauf M (2011) A description of the nonhydrostatic regional COSMO-Model—Part I: dynamics and numerics consortium for small-scale modelling. Deutscher Wetterdienst, Offenbach, Germany
- Fantini, A (2019) *Climate change impact on hazard over Italy*. PhD thesis, Università degli Studi di Trieste. URL <http://hdl.handle.net/11368/2940009>
- Flanner, M. G (2009) Integrating anthropogenic heat flux with global climate models. *Geophysical Research Letters*, 36(2), doi: <https://doi.org/10.1029/2008GL036465>.
- Förstner, J., Doms, G. (2004) Runge–Kutta time integration and high-order spatial discretization of advection - A new dynamical core for the LMK: Model development and application. *COSMO Newsletter* 4, 168–176, <http://www.cosmo-model.org/content/model/documentation/newsLetters/newsLetter04/chp9-6.pdf>.
- Fossler GSKPB, Khodayar S, Berg P (2015) Benefit of convection permitting climate model simulations in the representation of convective precipitation. *Clim Dyn* 44:45–60. <https://doi.org/10.1007/s00382-014-2242-1>
- Fowler HJ, Wasko C, Prein AF (2021) Intensification of short-duration rainfall extremes and implications for flood risk: current state of the art and future directions. *Phil Trans R Soc A* 379:20190541. <https://doi.org/10.1098/rsta.2019.0541>
- Fowler, H. J., Ali, H. (2022) Analysis of extreme rainfall events under the climatic change. In *Rainfall* (pp. 307–326). Elsevier, doi: <https://doi.org/10.1016/B978-0-12-822544-8.00017-2>.
- Garbero, V., Milelli, M., Bucchignani, E., Mercogliano, P., Varentsov, M., Rozinkina, I., ... Repola, F (2021) Evaluating the urban canopy scheme TERRA\_URB in the COSMO model for selected European cities. *Atmosphere*, 12, 237, doi: <https://doi.org/10.3390/atmos12020237>
- Gaume E, Bain V, Bernardara P, Newinger O, Barbuc M, Bateman A et al (2009) A compilation of data on European flash floods. *J Hydrol* 367(1–2):70–78. <https://doi.org/10.1016/j.jhydrol.2008.12.028>
- Giordani A, Cerenzia IML, Paccagnella T, Di Sabatino S (2023) SPHERA, a new convection-permitting regional reanalysis over Italy: Improving the description of heavy rainfall. *Q J R Meteorol Soc*. <https://doi.org/10.1002/qj.4428>
- Gustafsson, N., Berre, L., Hörnquist, S., Huang, X. Y., Lindskog, M., Navascues, B., ... & Thorsteinsson, S. (2001). Three-dimensional

- variational data assimilation for a limited area model: Part I: General formulation and the background error constraint. *Tellus A*, 53(4), 425–446, doi:<https://doi.org/10.1111/j.1600-0870.2001.00425.x>
- Gutowski, W.J., Ullrich, P.A., Hall, A., Leung, L. R., O'Brien, T.A., Patricola, C. M., ... Zarzycki, C (2020) The ongoing need for high resolution regional climate models: Process understanding and stakeholder information. *Bulletin of the American Meteorological Society*, 101, E664–E683, doi:<https://doi.org/10.1175/BAMS-D-19-0113.1>
- Haylock, M.R., Hofstra, N., Tank, A.K., Klok, E.J., Jones, P., New, M (2008) A European daily high-resolution gridded data set of surface temperature and precipitation for 1950–2006. *J. Geophys. Res. Space Phys.*, 113, doi: <https://doi.org/10.1029/2008JD010201>
- Hersbach, H., Bell, B., Berrisford, P., Hirahara, S., Horányi, A., Muñoz-Sabater, J., ... Thépaut, J. N (2020) The ERA5 global reanalysis. *Quarterly Journal of the Royal Meteorological Society*, 146, 1999–2049, doi:<https://doi.org/10.1002/qj.3803>
- Hohenegger C, Brockhaus P, Bretherton CS, Schär C (2009) The soil moisture-precipitation feedback in simulations with explicit and parameterized convection. *J Clim* 22:5003–5020. <https://doi.org/10.1175/2009JCLI2604.1>
- IPCC (2021). *Climate Change 2021: The Physical Science Basis*. Contribution of Working Group I to the Sixth Assessment Report of the Intergovernmental Panel on Climate Change. Masson-Delmotte, V., P. Zhai, A. Pirani, S.L. Connors, C. Péan, S. Berger, N. Caud, Y. Chen, L. Goldfarb, M.I. Gomis, M. Huang, K. Leitzell, E. Lonnoy, J.B.R. Matthews, T.K. Maycock, T. Waterfield, O. Yelekçi, R. Yu, and B. Zhou (eds.) Cambridge University Press, Cambridge, United Kingdom and New York, NY, USA, In press.
- Kappal, S. (2019). Data normalization using median median absolute deviation MMAD based Z-score for robust predictions vs. min–max normalization. *London Journal of Research in Science: Natural and Formal*. 19,4
- Karl TR, Nicholls N, Ghazi A (1999) CLIVAR/GCOS/WMO workshop on indices and indicators for climate extremes: Workshop summary. *Clim Change* 42:3–7
- Keller M, Fuhrer O, Schmidli J, Stengel M, Stöckli R, Schär C (2016) Evaluation of convection-resolving models using satellite data: The diurnal cycle of summer convection over the Alps. *Meteorol Z* 25:165–179. <https://doi.org/10.1127/metz/2015/0715>
- Kendon EJ, Prein AF, Senior CA, Stirling A (2021) Challenges and outlook for convection-permitting climate modelling. *Phil Trans R Soc A* 379:20190547. <https://doi.org/10.1098/rsta.2019.0547>
- Kjellström E, Boberg F, Castro M, Christensen JH, Nikulin G, Sánchez E (2010) Daily and monthly temperature and precipitation statistics as performance indicators for regional climate models. *Climate Research*, 44(2–3), 135–150, doi:10.3354/cr00932Lind, P., Lindstedt, D., Kjellström, E., Jones, C (2016) Spatial and temporal characteristics of summer precipitation over central Europe in a suite of high-resolution climate models. *J Clim* 29:3501–3518. <https://doi.org/10.1175/JCLI-D-15-0463.1>
- Koster RD, Dirmeyer PA, Guo Z et al (2004) Regions of strong coupling between soil moisture and precipitation. *Science* 305:1138–1140. <https://doi.org/10.1126/science.1100217>
- Leutwyler D, Imamovic A, Schär C. (2021) The continental-scale soil moisture-precipitation feedback in europe with parameterized and explicit convection. *J Clim* 34:5303–5320. doi: 10.1175/JCLI-D-20-0415.1Llasat, M., Llasat-Botija, M, Petrucci, O, Pasqua, A., Rosselló, J, Vinet, F, & Boissier, L, (2013) Towards a database on societal impact of Mediterranean floods within the framework of the HYMEX project. *Nat Hazard* 13(5):1337.
- Llasat MC, Llasat-Botija M, Prat M, Porcu F, Price C, Mugnai A et al (2010) High-impact floods and flash floods in Mediterranean countries: The FLASH preliminary database. *Adv Geosci* 23:47–55. <https://doi.org/10.5194/adgeo-23-47-2010>
- Lucas-Picher, P., Argüeso, D., Brisson, E., Trambly, Y., Berg, P., Lemonsu, A., ... Caillaud, C (2021) Convection-permitting modeling with regional climate models: Latest developments and next steps. *Wiley Interdisciplinary Reviews: Climate Change*, 12, e731, doi: <https://doi.org/10.1002/wcc.731>
- Maucha, G., Büttner, G., Kosztra, B. (2010) European validation of GMES FTS Soil Sealing Enhancement Data, Final Draft, Tech. rep., European Environmental Agency. [https://www.eea.europa.eu/data-and-maps/data/eea-fast-track-service-precursor-on-land-monitoring-degree-of-soil-sealing/eea-ftsp-degree-of-soil-sealing-1/soilsealing\\_european\\_validation\\_finaldraft2t.pdf/download](https://www.eea.europa.eu/data-and-maps/data/eea-fast-track-service-precursor-on-land-monitoring-degree-of-soil-sealing/eea-ftsp-degree-of-soil-sealing-1/soilsealing_european_validation_finaldraft2t.pdf/download)
- McCabe GJ, Markstrom SL (2007) A monthly water-balance model driven by a graphical user interface, Vol. 1088, US Geological Survey Reston, VA.Mellor, G. L., Yamada T (1982) Development of a turbulence closure model for geophysical fluid problems. *Rev Geophys* 20:851–875. <https://doi.org/10.1029/RG020i004p00851>
- Miglietta MM, Davolio S (2022) Dynamical forcings in heavy precipitation events over Italy: lessons from the HyMeX SOP1 campaign. *Hydrol Earth Syst Sci* 26(3):627–646. <https://doi.org/10.5194/hess-26-627-2022>
- Milovac J, Warrach-Sagi K, Behrendt A, Späth F, Ingwersen J, Wulfmeyer V (2016) Investigation of PBL schemes combining the WRF model simulations with scanning water vapor differential absorption lidar measurements. *J Geophys Res Atmos* 121:624–649. <https://doi.org/10.1002/2015JD023927>
- Monteiro D, Caillaud C, Samacoïts R, Lafaysse M, Morin S (2022) Potential and limitations of convection-permitting CNRM-AROME climate modelling in the French Alps. *Int J Climatol*. <https://doi.org/10.1002/joc.7637>
- Müller, S. K., Caillaud, C., Chan, S., de Vries, H., Bastin, S., Berthou, S., ... & Warrach-Sagi, K (2022) Correction to: Evaluation of Alpine-Mediterranean precipitation events in convection-permitting regional climate models using a set of tracking algorithms. *Climate Dynamics*, 1–1, doi: <https://doi.org/10.1007/s00382-022-06555-z>
- Oke, T. R., Mills, G., Christen, A., Voogt, J. A. (2017) *Urban climates*. Cambridge Press.
- Patro, S., Sahu, K. K (2015) Normalization: A preprocessing stage. *arXiv preprint arXiv:1503.06462*
- Perkins SE, Pitman AJ, Holbrook NJ, McAneney J (2007) Evaluation of the AR4 climate models' simulated daily maximum temperature, minimum temperature, and precipitation over Australia using probability density functions. *J Clim* 20(17):4356–4376. <https://doi.org/10.1175/JCLI4253.1>
- Piazza M, Prein AF, Truhetz H, Csaki A (2019) On the sensitivity of precipitation in convection-permitting climate simulations in the Eastern Alpine region. *Meteorol Z* 28:323–346. <https://doi.org/10.1127/metz/2019/0941>
- Pichelli E, Coppola E, Sobolowski S, Ban N, Giorgi F, Stocchi P, Alias A, Belušić D, Berthou S, Caillaud C, Cardoso RM, Chan S, Christensen Ole B, Dobler A, de Vries H, Goergen K, Kendon EJ, Keuler K, Geert L, Lorenz T, Mishra AN, Panitz HJ, Schär C, Soares PM, Truhetz H, Vergara-Temprado J (2021) The first multi-model ensemble of regional climate simulations at kilometer-scale resolution part 2: historical and future simulations of precipitation. *Clim Dyn* 56(11–12):3581–3602. <https://doi.org/10.1007/s00382-021-05657-4>
- Pielke RA (2001) Influence of the spatial distribution of vegetation and soils on the prediction of cumulus convective rainfall. *Rev Geophys* 39:151–177. <https://doi.org/10.1029/1999RG000072>
- Pilguy, N., Taszarek, M., Kryza, M., Brooks, H (2022) Reconstruction of Violent Tornado Environments in Europe: High-Resolution Dynamical Downscaling of ERA5. *Geophysical Research Letters*, e2022GL098242, doi: <https://doi.org/10.1029/2022GL098242>



- Prein AF, Gobiet A, Suklitsch M, Truhetz H, Awan NK, Keuler K, Georgievski G (2013) Added value of convection permitting seasonal simulations. *Clim Dyn* 41:2655–2677. <https://doi.org/10.1007/s00382-013-1744-6>
- Raffa M, Reder A, Marras GF, Mancini M, Scipione G, Santini M, Mercogliano P (2021a) VHR-REA\_IT Dataset: Very High Resolution Dynamical Downscaling of ERA5 Reanalysis over Italy by COSMO-CLM. *Data* 6(8):88. [https://doi.org/10.3390/data6080088\(a\)](https://doi.org/10.3390/data6080088(a))
- Raffa, M., Reder, A., Adinolfi, M., Mercogliano, P (2021b) A comparison between one-step and two-step nesting strategy in the dynamical downscaling of regional climate model COSMO-CLM at 2.2 km driven by ERA5 reanalysis. *Atmosphere*, 12, 260, doi:<https://doi.org/10.3390/atmos12020260> (b)
- Raschendorfer, M (2001) The new turbulence parameterization of LM. COSMO Newsletter 1, 89–97, [http://www.cosmo-model.org/content/model/documentation/newsLetters/newsLetter01/newsLetter\\_01.pdf](http://www.cosmo-model.org/content/model/documentation/newsLetters/newsLetter01/newsLetter_01.pdf)
- Reder A, Rianna G (2021) Exploring ERA5 Reanalysis Potentialities for Supporting Landslide Investigations: A Test Case from Campania Region (Southern Italy). *Landslides* 18:1909–1924. <https://doi.org/10.1007/s10346-020-01610-4>
- Reder A, Rianna G, Mercogliano P, Castellari S (2018) Parametric investigation of Urban Heat Island dynamics through TEB 1D model for a case study: Assessment of adaptation measures. *Sustain Cities Soc* 39:662–673. <https://doi.org/10.1016/j.scs.2018.03.023>
- Reder A, Raffa M, Montesarchio M, Mercogliano P (2020) Performance evaluation of regional climate model simulations at different spatial and temporal scales over the complex orography area of the Alpine region. *Nat Hazards* 102:151–177. <https://doi.org/10.1007/s11069-020-03916-x>
- Reder, A., Raffa, M., Padulano, R., Rianna, G., Mercogliano, P (2022) Characterizing extreme values of precipitation at very high resolution: An experiment over twenty European cities. *Weather and Climate Extremes*, 35, 100407, doi:<https://doi.org/10.1016/j.wace.2022.100407>.
- Ridal, M., Olsson, E., Unden, P., Zimmermann, K., Ohlsson, A (2017) Uncertainties in Ensembles of Regional Re-Analyses. Deliverable D2.7 HARMONIE Reanalysis Report of Results and Dataset. Available online: <http://www.uerra.eu/component/dpattachments/?task=attachment.download&id=296>
- Ritter B, Geleyn JF (1992) A comprehensive radiation scheme for numerical weather prediction models with potential applications in climate simulations. *Mon Wea Rev* 120:303–325. [https://doi.org/10.1175/1520-0493\(1992\)120%3c0303:ACRSFN%3e2.0.CO;2](https://doi.org/10.1175/1520-0493(1992)120%3c0303:ACRSFN%3e2.0.CO;2)
- Rockel B, Will A, Hense A (2008) The regional climate model COSMO-CLM (CCLM). *Meteorol Z* 17:347–348. <https://doi.org/10.1127/0941-2948/2008/0309>
- Sangelantoni L, Sobolowski S, Lorenz T, Hodnebrog Ø, Cardoso RM, Soares P, Ferretti R, Lavín-Gullón A, Fernandez J, Goergen K, Milovac J, Katragkou E, Kartsios S, Coppola E, Pichelli E, Adinolfi M, Mercogliano P, Berthou S, de Vries H, Dobler A, Belušić A, Feldmann H, Tölle M, Bastin S (2023) Investigating the representation of heatwaves from an ensemble of km-scale regional climate simulations within CORDEX-FPS convection. *Clim Dyn*. <https://doi.org/10.1007/s00382-023-06769-9>
- Schär C, Ban N, Fischer EM, Rajczak J, Schmidli J, Frei C, O’Gorman P (2016) Percentile indices for assessing changes in heavy precipitation events. *Clim Change* 137(1–2):201–216. <https://doi.org/10.1007/s10584-016-1669-2>
- Schrodin, R., Heise, E.(2001). The Multi-Layer Version of the DWD Soil Model TERRA-LM, COSMO Tech. Rep., 2, <https://www.cosmo-model.org/content/model/cosmo/techReports/docs/techReport02.pdf>
- Soares PM, Cardoso RM (2018) A simple method to assess the added value using high-resolution climate distributions: application to the EURO-CORDEX daily precipitation. *Int J Climatol* 38(3):1484–1498. <https://doi.org/10.1002/joc.5261>
- Soares, P. M. M., Careto, J. A. M., Cardoso, R. M., Goergen, K., Katragkou, E., Sobolowski, S., ... & Bastin, S. (2022). The added value of km-scale simulations to describe temperature over complex orography: the CORDEX FPS-Convection multi-model ensemble runs over the Alps. *Climate Dynamics*, 1–24. doi:<https://doi.org/10.1007/s00382-022-06593-7>
- Taylor CM, Birch CE, Parker DJ et al (2013) Modeling soil moisture-precipitation feedback in the Sahel: Importance of spatial scale versus convective parameterization. *Geophys Res Lett* 40:6213–6218. <https://doi.org/10.1002/2013GL058511>
- Thornthwaite CW, Mather JR (1955) The water balance. Publications in climatology, Laboratory of Climatology, p 8
- Tiedtke M (1989) A comprehensive mass flux scheme for cumulus parameterization in large-scale models. *Mon Weather Rev* 117:1779–1800. [https://doi.org/10.1175/1520-0493\(1989\)117%3c1779:ACMFSF%3e2.0.CO;2](https://doi.org/10.1175/1520-0493(1989)117%3c1779:ACMFSF%3e2.0.CO;2)
- Tölle, M. H., & Churilun, E., (2021) Sensitivity of Convection-Permitting Regional Climate Simulations to Changes in Land Cover Input Data: Role of Land Surface Characteristics for Temperature and Climate Extremes. *Frontiers in Earth Science*, 9, 722244. doi: <https://doi.org/10.3389/feart.2021.722244>
- Wackernagel, H. (1995) Ordinary Kriging. In: *Multivariate Geostatistics*. Springer, Berlin, Heidelberg, doi:[https://doi.org/10.1007/978-3-662-03098-1\\_11](https://doi.org/10.1007/978-3-662-03098-1_11)
- Wang X, Tolksdorf V, Otto M, Scherer D (2021) WRF-based dynamical downscaling of ERA5 reanalysis data for High Mountain Asia: Towards a new version of the High Asia Refined analysis. *Int J Climatol* 41:743–762. <https://doi.org/10.1002/joc.6686>
- Wouters H, Demuzere M, Blahak U, Fortuniak K, Maiheu B, Camps J, Tieleman D, van Lipzig NPM (2016) The efficient urban canopy dependency parametrization (SURY) v1.0 for atmospheric modeling: Description and application with the COSMO-CLM model for a Belgian summer. *Geosci Model Dev* 9:3027–3054. <https://doi.org/10.5194/gmd-9-3027-2016>
- Yang L, Sun G, Zhi L, Zhao J (2018) Negative soil moisture-precipitation feedback in dry and wet regions. *Sci Rep* 8:1–9. <https://doi.org/10.1038/s41598-018-22394-7>
- Zittis G, Bruggeman A, Camera C, Hadjinicolaou P, Lelieveld J (2017) The added value of convection permitting simulations of extreme precipitation events over the eastern Mediterranean. *Atmos Res* 191:20–33. <https://doi.org/10.1016/j.atmosres.2017.03.002>
- Zollo AL, Rillo V, Bucchignani E, Montesarchio M, Mercogliano P (2016) Extreme temperature and precipitation events over Italy: assessment of high-resolution simulations with COSMO-CLM and future scenarios. *Int J Climatol* 36:987–1004. <https://doi.org/10.1002/joc.4401>

**Publisher's Note** Springer Nature remains neutral with regard to jurisdictional claims in published maps and institutional affiliations.